The United Nations University

GEOTHERMAL TRAINING PROGRAMME
Orkustofnun, Grensásvegur 9,
IS-108 Reykjavík, Iceland

Reports 1995
Number 15

# RESERVOIR ASSESSMENT OF THE SUDURHLÍDAR GEOTHERMAL FIELD IN KRAFLA, NE-ICELAND

**Xu Shiguang**
Yunnan Geological Engineering Survey Institute,
650041 Dongjiawan, Kunming,
P.R. CHINA

## ABSTRACT

The Sudurhlídar geothermal field is the eastern part of the Krafla geothermal area in Northeast Iceland. Six wells were drilled in the Sudurhlídar field in the period 1980-1982. Five of the wells were productive and are connected to the Krafla power plant. Temperature and pressure logs from the wells have been analysed and formation temperature and initial pressure profiles estimated. Based on this work a natural conceptual model has been put forward. The model assumes that the reservoir is bounded by impermeable faults to the west and to the east. Recharge of approximately 250°C hot water is predicted to be into the southeastern part of the well field, below 1 km depth. Near the recharge zone the reservoir is in subcooled liquid conditions but further away, boiling conditions prevail from surface to at least 2.2 km depth.

Lumped modelling was applied to study and predict the behaviour of the reservoir during exploitation. The generating capacity of the system was assessed by using volumetric methods. The lumped modelling suggests a reservoir area of 10 $km^2$ and the volumetric assessment gives a 15-35 $MW_e$ power potential for a reservoir area of 3 $km^2$, and 30-70 $MW_e$ for a possible area of 7 $km^2$.

## 1. INTRODUCTION

The Krafla geothermal area is situated in one of the five distinct volcanic systems with fissure swarms in the neovolcanic zone in NE-Iceland (Figure 1). These are part of the surface expressions of the Mid-Atlantic Ridge in Iceland. The volcanic activity at Krafla is episodic, occurring every 250-1000 years, and each episode lasting 10-20 years. The latest eruptive period started in 1975 and terminated in September 1984. The Krafla central volcano developed a caldera during the last interglacial period about 100 thousand years ago which has since almost been filled with volcanic material. Within the caldera there are numerous fumaroles and hot and altered grounds that are mostly connected to tectonic fractures and faults. These geothermal manifestations indicate the existence of a large geothermal system. The exploration of this system began in 1970 (Stefánsson, 1981; Bödvarsson et al., 1984; Ármannsson et al., 1987).


FIGURE 1: A tectonic map of the Krafla area (Ármannsson et al., 1987)

## 1.1 Exploration history

**Surface exploration:** Early investigation included geological mapping, an aeromagnetic survey, resistivity measurements, gravity mapping and chemical analysis of the fumarole gases and fluids. Later work included more extensive geological mapping along with more detailed resistivity and ground magnetic surveys of specific drilling fields (Ármannsson et al., 1987). The general results of the gelogical exploration are summarized in Figures 1 and 2.

**Subsurface exploration:** Drilling in Krafla started in 1974 with two 1200 m deep exploration wells. Three production wells were drilled in 1975 and by the year 1978 12 wells had been completed, all of which were in the Leirbotnar field, to the west of the Hveragil gully (Figure 2) . In 1976 the reservoir fluid at Leirbotnar field became contaminated with magmatic gases causing depositions and corrosion in the wells with a simultaneous decline in their productivity. In 1980 drilling continued with two production wells in the Leirbotnar field and one exploration well in Sudurhlídar, in the eastern part of the Krafla geothermal area. This well showed that the reservoir in the east was not affected by the magmatic activity, which was in agreement with the chemical studies of the fumaroles in Sudurhlídar. Thus, from 1981 to 1982 five wells were drilled in the Sudurhlídar field (the name meaning the southern slopes of Mt. Krafla). Since 1982 no additional wells have been drilled in Sudurhlídar. The basic data of the wells in the Sudurhlídar field are summarized in Table 1.

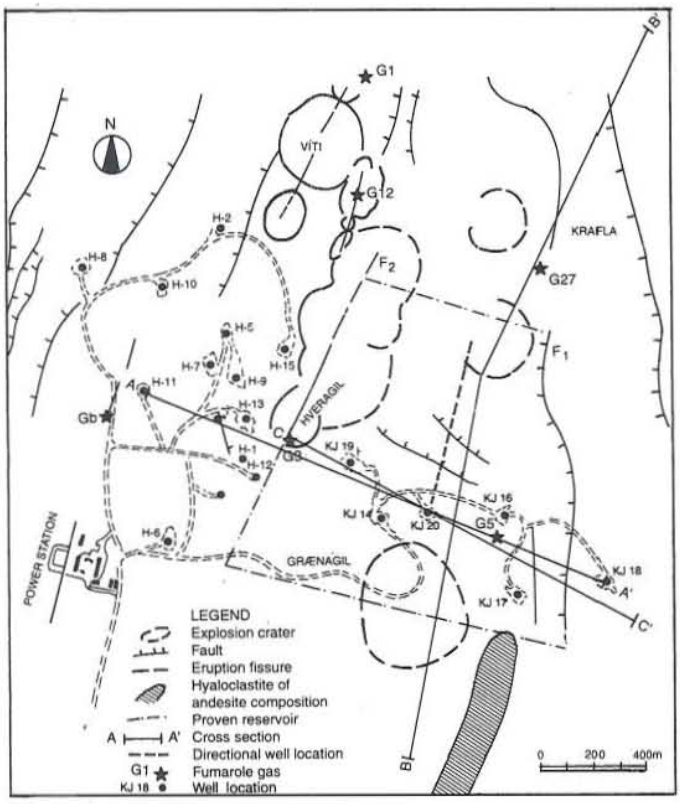


FIGURE 2: A schematic geological map and location of wells in the Sudurhlídar field (Ármannsson et al., 1989)

## 1.2 Lithology and tectonics

The surface of the Krafla area is mostly covered with basaltic lavas, along with a little hyaloclastite of andesite composition as shown in Figure 2. The investigations of subsurface lithology are based on the analysis of drill cuttings from all wells in Krafla. Information has been obtained on the geological structure, the distribution of individual lithological units, the correlation of aquifers with them and the degree of rock alteration (Ármannsson et al., 1987). A geological cross-section A-A´ is shown in Figure 3 (location see Figure 2).

TABLE 1: Basic data for the wells in the Sudurhlídar geothermal field

| Well No. Elevation (m a.s.l.) Depth (m) | Drilling depth | | Diameter | | Drillbit diameter (mm) | Locations of feed-zones in production part of well (m) | | Year drilled |
|---|---|---|---|---|---|---|---|---|
| | From (m) | To (m) | Casing (") | Liner (") | | | | |
| **KJ 14** | 0 | 61 | 18 5/8 | | 584 | 850 | 1050 | 1980 |
| | 0 | 210 | 13 3/8 | | 445 | 1250 | 1785 | |
| 571.07 | 0 | 705 | 9 5/8 | | 311 | 1834 | 2087 | |
| 2107 | 679 | 1527 | | 7 5/8 | 216 | | | |
| | 1527 | 2099 | | 7 | 216 | | | |
| **KJ 16** | 0 | 60 | 18 5/8 | | 559 | 805 | 850-900 | 1981 |
| | 0 | 210 | 13 3/8 | | 444 | 935 | 1075 | |
| 609.5 | 0 | 647 | 9 5/8 | | 311 | 1150 | 1790 | |
| 1981 | 624 | 1836 | | 7 5/8 | 216 | 1970 | | |
| | 1836 | 1951 | | 7 | 216 | | | |
| **KJ 17** | 0 | 65 | 18 | | 559 | 800 | 950-1000 | 1981 |
| | 0 | 212 | 13 3/8 | | 444 | 1085 | 1110 | |
| 643.0 | 0 | 695 | 9 5/8 | | 311 | 1120 | 1600 | |
| 2190 | 642 | 1964 | | 7 5/8 | 216 | 1850 | | |
| **KJ 18** | 0 | 559 | 18 5/8 | | 559 | 750 | 900 | 1981 |
| | 0 | 206 | 13 3/8 | | 444 | 1710 | 2200 | |
| 611.5 | 0 | 674 | 9 5/8 | | 311 | | | |
| 2215 | 669 | 2215 | | 7 5/8 | 216 | | | |
| **KJ 19** | 0 | 65 | 18 5/8 | | 559 | 830 | 925 | 1982 |
| | 0 | 203 | 13 3/8 | | 444 | 995 | 1190 | |
| 584.0 | 0 | 654 | 9 5/8 | | 311 | 1895 | 1920 | |
| 2150 | 495 | 2009 | | 7 | 216 | | | |
| **KJ 20** | 0 | 63 | 18 5/8 | | 559 | 720 | 935-960 | 1982 |
| | 0 | 212 | 13 3/8 | | 444 | 1055 | 1100-1200 | |
| 584.5 | 0 | 650 | 9 5/8 | | 311 | 1270 | 1300-1500 | |
| 1823 | 604 | 1770 | | 7 | 216 | 1645 | 1720 | |
| | | | | | | | 1760 | |

The faults in the field are controlled and affected by the active fissure swarm mentioned earlier and extend mainly from north-northeast to south-southwest or nearly in a N-S direction with steep dip angles (Figure 3). Exceptions from this are two small faults in the north of the Sudurhlídar well field which extend from southeast to northwest (Figure 2).

### 1.3 Geophysics

Resistivity surveys are among the most powerful methods in geothermal exploration in Iceland (Árnason and Flóvenz, 1992). The Schlumberger DC resistivity method has mainly been used in the Krafla field,

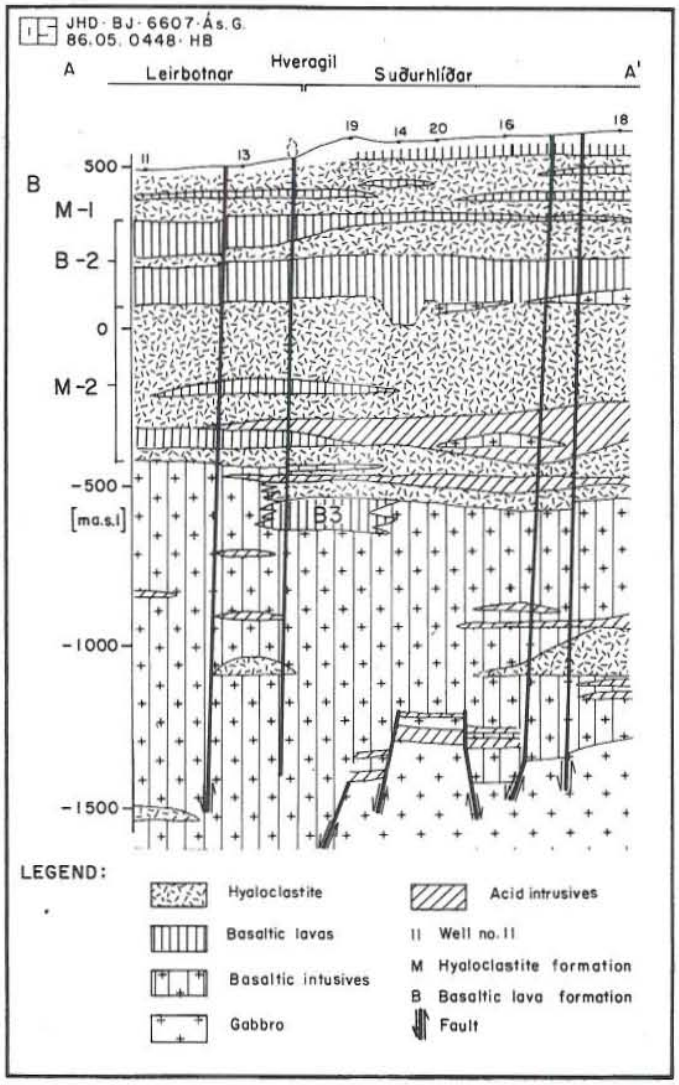


but several dipole soundings, TEM and magnetotelluric measurements have been carried out as well. Based on the relationship between the bulk resistivity and the type of the alteration minerals which indicate the temperature at a certain depth, the extensive N-S cross-section B-B´ shown in Figure 2 is presented in Figure 4 (Árnason and Karlsdóttir, 1995). It defines the north and sourth boundaries of the reservoir. The geothermal system is represented by the layer of resistivity less than 10 Ωm and the high- resistivity core under the low-resistivity layer.

FIGURE 3: Lithological cross-section A-A' through the Krafla area, for location see Figure 2 (Ármannsson et al., 1987)

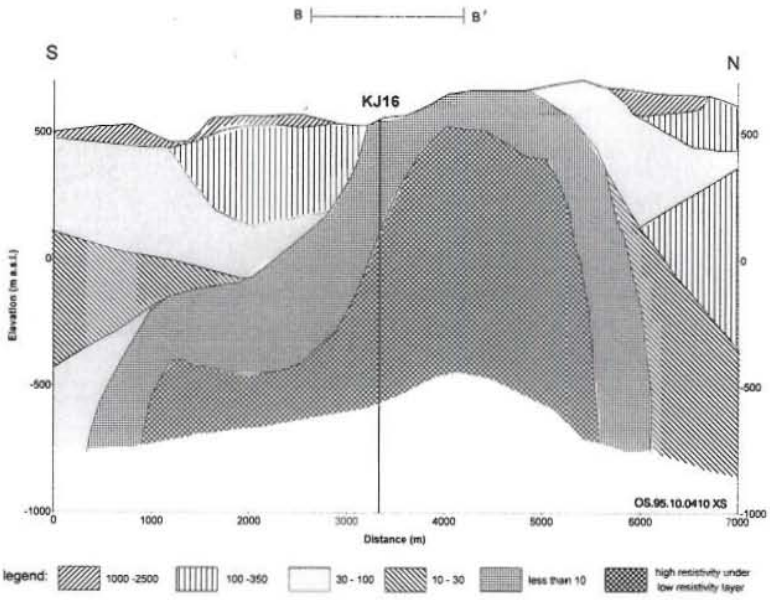


FIGURE 4: Resistivity cross-section B-B' (values in Ωm), location is shown in Figure 2 (Árnason and Karlsdóttir, 1995)

## 2. A CONCEPTUAL RESERVOIR MODEL

The reservoir of the Sudurhlídar field is in the natural state filled mostly with liquid-dominant boiling fluid in its fractures (Bödvarsson et al., 1984). It is difficult to evaluate the formation temperature from temperature data just after drilling of the wells due to the fluid circulation during drilling and the large quantity of cold water injected into the wells during tests. Rapid thermal recovery after drilling and boiling within wells also limits the possibilities in obtaining useful information for interpreting formation temperature. The data however, become more reliable as time passes. The Sudurhlídar field has been monitored by annual temperature and pressure surveys in some wells during the 10-15 years of exploitation.

### 2.1 Caprock

Surface geothermal activity in the Sudurhlídar field is limited to fumaroles and steaming grounds, hot springs are absent. However, the mixture of liquid water and steam rushing outt from the production wells, indicates the existence of caprock. Both lithology and resistivity in the field indicate thin caprock characteristics. The caprock thickness in each well is given in Table 2, based chiefly on the lithological interpretation.

TABLE 2: Caprock thickness in the Sudurhlídar wells

| | KJ14 | KJ16 | KJ17 | KJ18 | KJ19 | KJ20 |
|---|---|---|---|---|---|---|
| Thickness (m) | 50 | 60 | 60 | 70 | 70 | 60 |
| Lower boundary (m a.s.l.) | 520 | 550 | 580 | 540 | 515 | 540 |

### 2.2 Pressure pivot point analysis

A pronounced pivot point was seen in pressure logs in wells KJ14, KJ16, KJ19 and KJ20 during the warming up period after drilling of the wells (Figure 5). The pivot point pressure indicates the initial conditions in the respective wellat the depth of the pivot point. This conclusion is also confirmed by the fact that the major feedzones coincide with the pivot point locations respectively in wells KJ14, KJ16, KJ19 and KJ20.

### 2.3 Formation temperature analysis

With regards to the relatively homogeneous caprock thermal conductivity, a straight line which connects the temperature value at the top of the reservoir with the mean annual surface temperature for Krafla area, i.e. 5°C, is used to evaluate caprock temperatures in each well.

KJ14 warmed up so rapidly that it was put into production less than one month after completion of drilling. The highest temperature, 290.1°C, was measured at the pivot point at 1020 m depth. The temperature should go a little higher if there was no inevitable pressure draw-down caused by the discharge. Comparing the temperature value with the initial pressure at the major feedzone (the pivot point), confirms boiling conditions in the reservoir. Therefore, below the caprock depth a boiling curve is employed as the formation temperature profile for well KJ14 as shown in Figure 6A. Some downhole temperature data above the feedzone fit the boiling point depth curve very well, while the measurements close to the well bottom seem to be relatively low. This is due to the fact that the well was flowing at low internal pressure just before the measured data was collected.

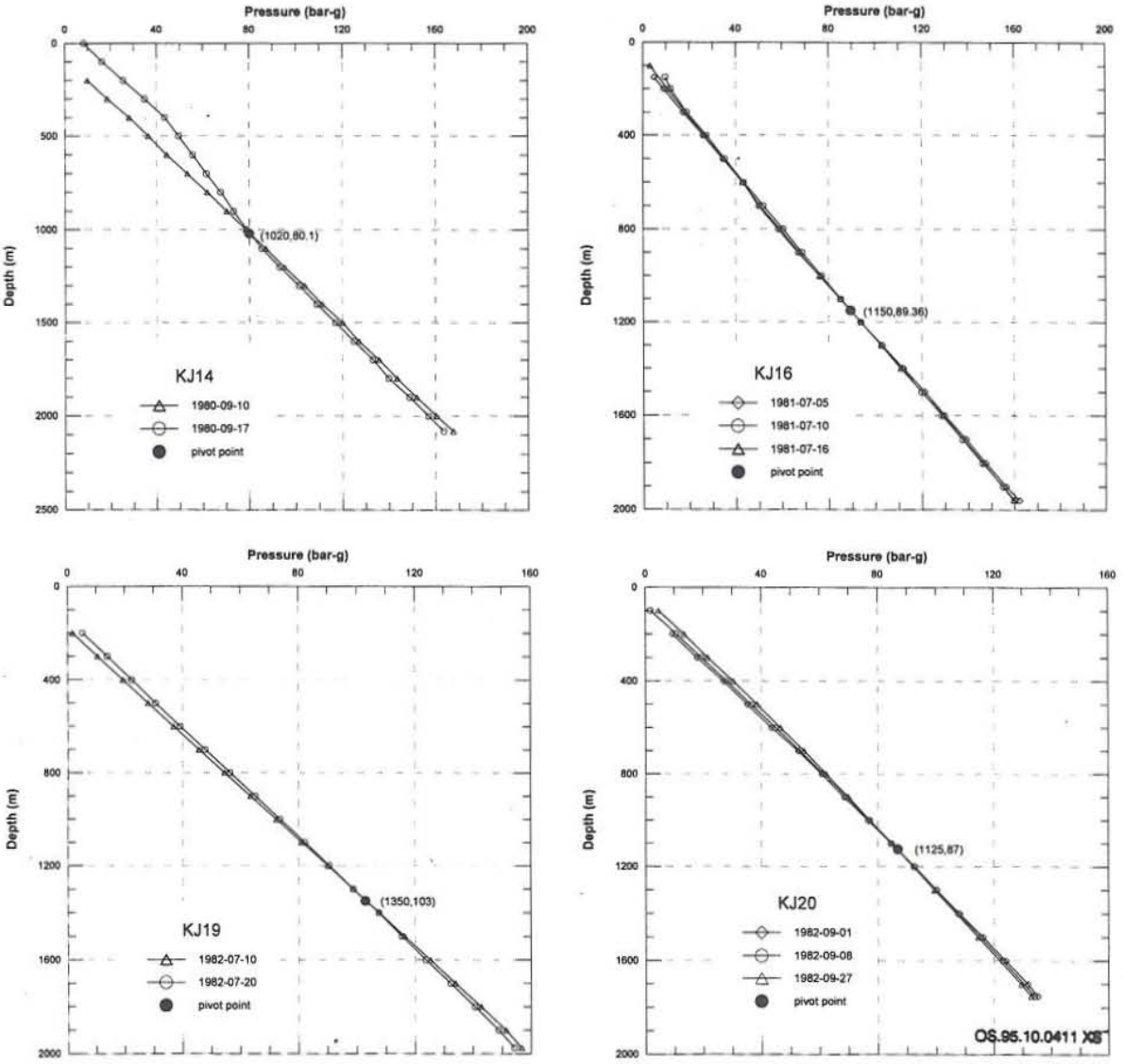


FIGURE 5: Pressure pivot point in the wells of the Sudurhlídar field

Comparing the measured temperature of 290.9°C at the major feedzone of well KJ16 thirteen years after completion, with the corresponding pressure at the same time, 83.31 bar-g, a boiling nature of the neighbouring reservoir is also likely. When a boiling curve has been used to match the measured data 13 years later, the good fit verifies the boiling guess (Figure 6B). By simply shifting the boiling curve to fit the temperature that corresponds to the initial pressure on the boiling curve, the reservoir temperature above the major feedzone has been achieved. Below the major feedzone at 1150 m depth, the temperature is significantly lower than the boiling curve and has been stable for 14 years (Figure 7). This proves that the geothermal system is in a water-phase at the deeper parts of well KJ16 and pressure draw-down will therefore not greatly affect reservoir temperatures. The formation temperature is then evaluated by plotting the temperature history at certain depths as shown in Figure 7. Smoothing the estimated points, a complete formation temperature profile in KJ16 has been established (Figure 6B).

There was no pressure pivot point observed in well KJ17, but it shows similar temperature conditions as in well KJ16. Both of the wells are located near the fault $F_1$ (see Figure 2) that can be considered as the eastern boundary of the Sudurhlídar field (see also Chapter 2.4), and the temperature in both wells increases monotonously with depth above 1000-1200 m depth, but drops and fluctuates as going deeper. Therefore similar formation temperature profiles are estimated for wells KJ16 and KJ17. Actually, when the same boiling curve has been applied here, some measurements, which also would be higher if there

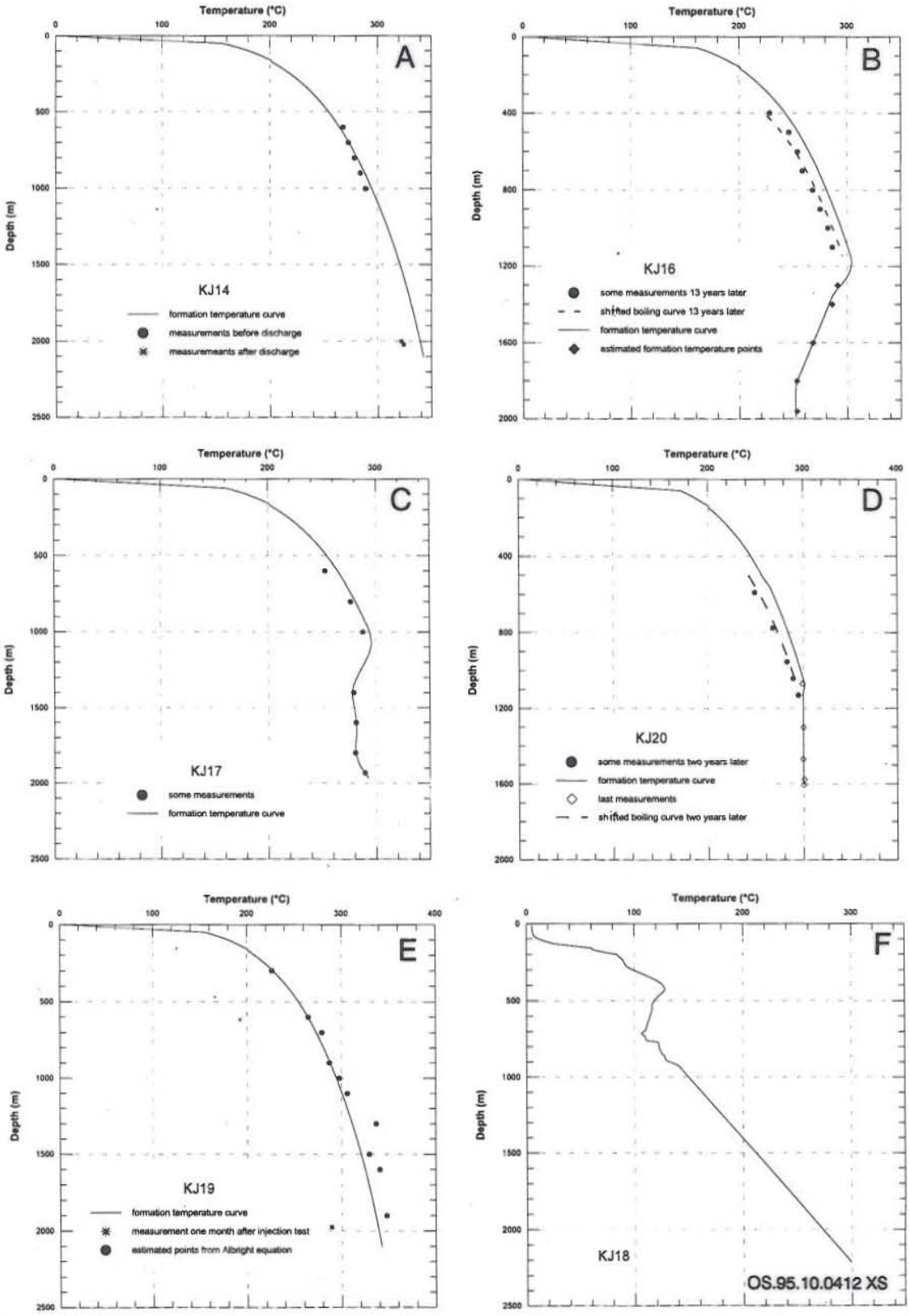


FIGURE 6: Formation temperature profiles in the Sudurhlídar wells

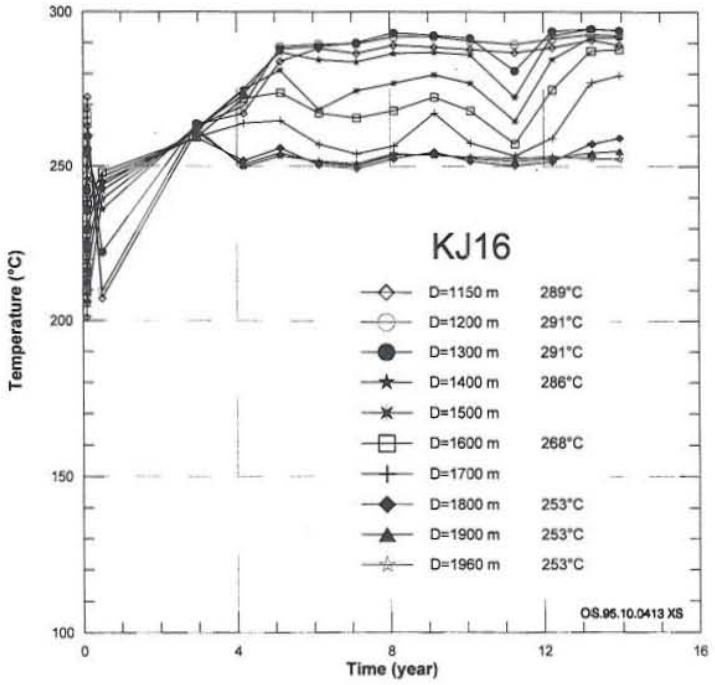


FIGURE 7: Temperature history at several depths in well KJ-16

were no pressure draw-down, confirm the evaluation (Figure 6C). For the liquid system under the major feedzone (950-1000 m), where the highest temperature with the value of 295.6°C was recorded, the latest observed data have been used to complete the formation profile for KJ17.

To evaluate the formation temperature for well KJ20, above the major feedzone the same principle was used as for KJ16, and in the deeper part the same principle as for KJ17. The result is shown in Figure 6D. In the upper part of the well a perfect fit of the boiling curve, that is shifted to correspond to pressure at the major feedzone 2 years later with the measurements at the same time, confirms the evaluation. As this is a directional well, some measured depth data have been modified to obtain true vertical depths.

Well KJ19 was only logged during the first month after completion. A boiling curve with depth is suggested for the well, intersecting the pivot point at 1350 m. Fortunately, the recovery temperature was so regular that the Albright equation (Helgason, 1993) can be used to estimate the formation temperature (see Appendix I). As this method usually gives a value on the high side, it is not surprising to have the boiling curve formation temperature profile as shown in Figure 6E. The measured temperature near the bottom after one month's warming up, which similarly should go up, most likely agrees with the evaluation.

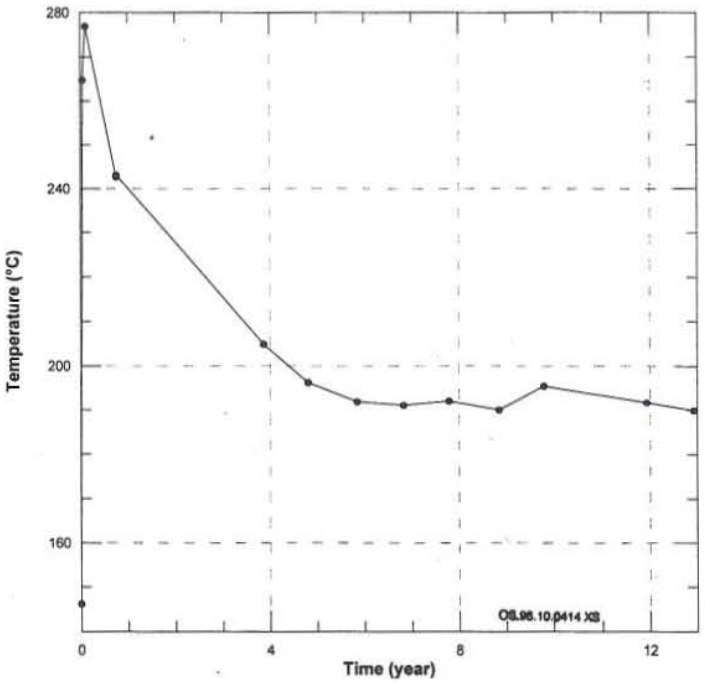


FIGURE 8: Temperature history at 2180 m depth in KJ-18

As KJ18 is located to the east of the fault $F_1$ which forms the eastern boundary of the Sudurhlídar field, it shows very different temperature conditions. Above 980 m depth the temperature has been steady for thirteen years and therefore represents the true formation temperature. At the bottom the temperature once reached 277°C just twenty days after drilling. Due to down-flow in the well from an aquifer at about 1000 m depth, the temperature at the bottom has dropped to less than 200°C (Figure 8). The formation temperature at the bottom is therefore estimated as 300°C and is increasing linearly from 1000 m depth (Figure 6F).

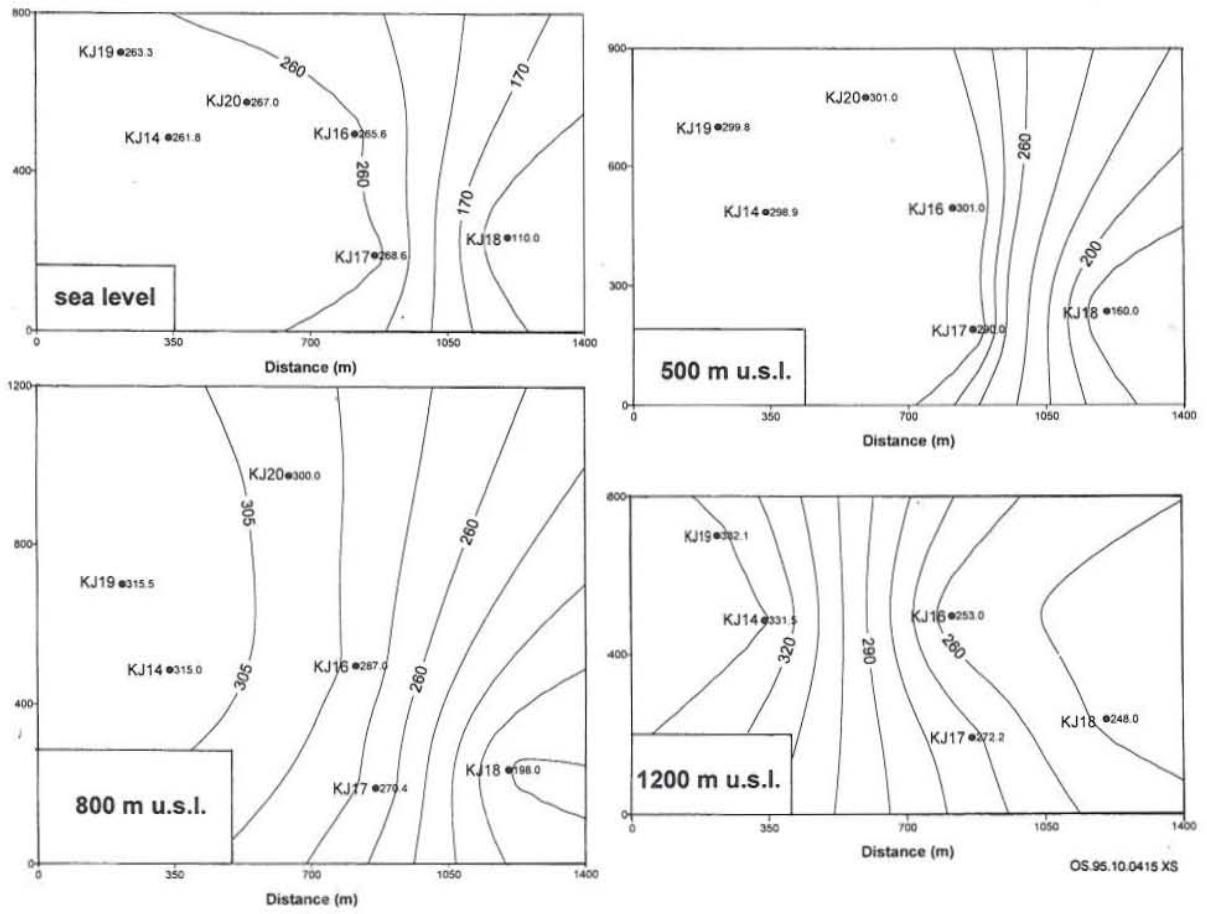


FIGURE 9: Iso-maps of the formation temperature in the Sudurhlídar field

Figure 9 presents four temperature contour maps at different elevation. They show that the reservoir temperature in the east part of the well field, i.e. east of the fault $F_1$, is substantially lower than in the west. However, below 1200 m u.s.l., this lateral temperature gradient appears to vanish. The temperature distribution to the west of $F_1$ at the same level is uniform above 500 m u.s.l. However, due to the different phase character as going down, the western part of the well field (KJ14 and KJ19, boiling phase) is much hotter than the central part (KJ16 and KJ17, water phase). Figure 10A shows the temperature distribution in the cross-section C-C′, shown in Figure 2, together with the location of feedzones beneath the production casings.

## 2.4 Initial reservoir pressure

The Sudurhlídar wells can be classified into three groups. These are wells intersecting only the boiling reservoir, wells that penetrate the boiling reservoir and continue into the water-phase system below, and wells only intersecting the water-phase reservoir. The liquid-dominated boiling reservoir conditions are defined in terms of pressure and temperature by using the boiling curve with depth analysis (Arason and Björnsson, 1994):

$$P(z) = P_0 + g \int_0^z \rho_{sat}\, dz \qquad (1)$$

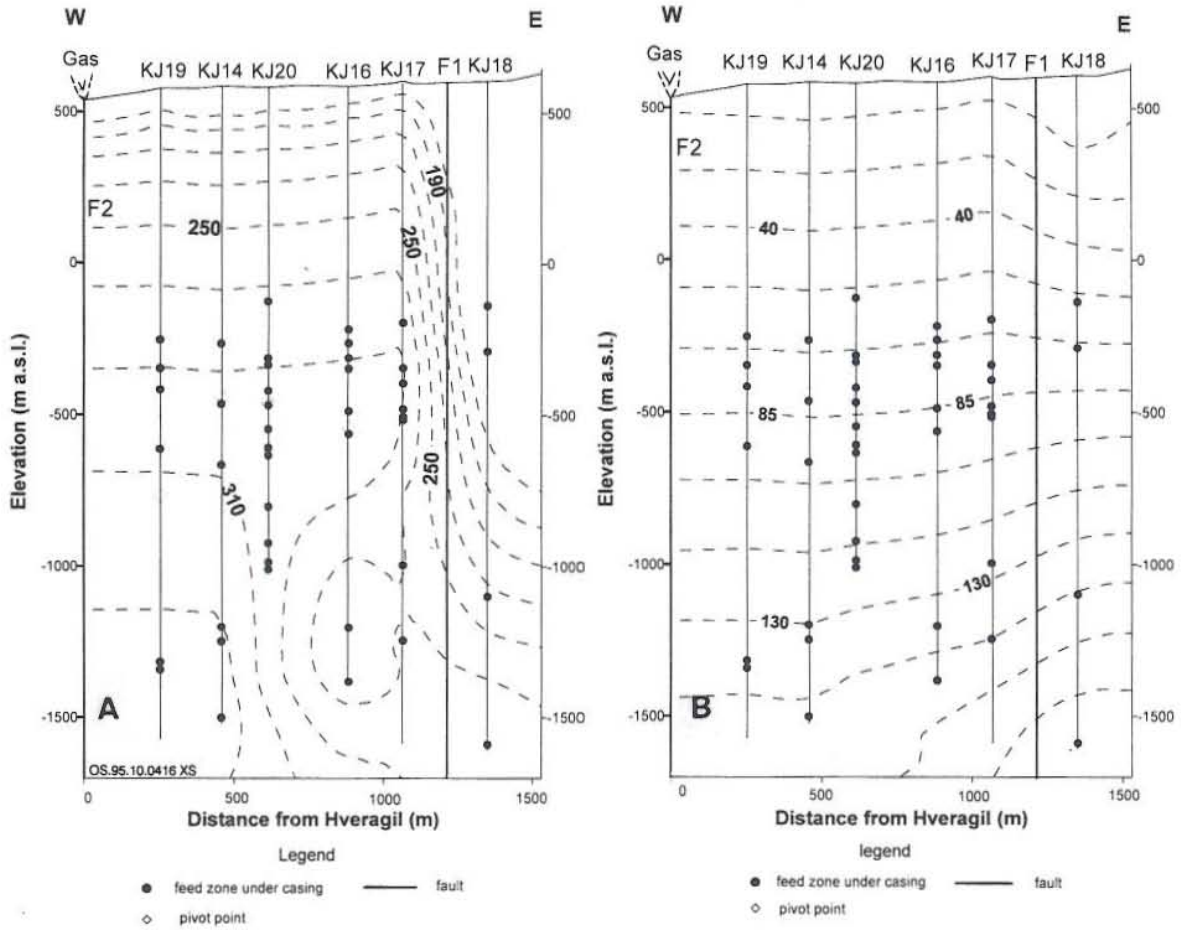


FIGURE 10: Cross-section C-C' through the Krafla system, a) Temperature distribution, b) pressure distribution; location is shown in Figure 2

where

$P(z)$ = Pressure at any depth z (bar-g);
$P_0$ = Pressure at a certain initial elevation $z_0$ (bar-g);
$g$ = Acceleration of gravity (m/s$^2$);
$z$ = Depth of the calculated pressure (m);
$\rho_{sat}$ = Density of water at saturation pressure (kg/m$^3$).

The equation is nonlinear and solved numerically to fit the pivot pressure value that was observed for the boiling wells (see Figure 5). Wells KJ16, KJ17 and KJ20 also have their pivot points at boiling conditions, therefore the boiling curve with depth analysis applies as an initial reservoir temperature and pressure estimate down to the depth of the major feedzone. However, at greater depth water-phase conditions take over, resulting in an initial pressure estimate which is simply based on a similar equation as Equation 1

$$P(z) = P_p + g \int_{D_p}^{D_T} \rho_l(T(z))\, dz \qquad (2)$$

where

$P_p$ = Pressure at the pivot point (bar-g);
$D_T$ = Total depth of the well (m);
$D_p$ = Depth to the pivot point (m);
$\rho_l$ (T(z)) = Water density at the formation temperature T(z) (kg/m$^3$).

In KJ18 the first pressure logging after drilling is used as its initial pressure. The pressure maps in Figure 11 show that at sea level the pressure west of fault $F_1$ is higher than in the east, while at 500 m u.s.l. they tend to be equal, but reversed deeper. At 1200 m u.s.l. a 14 bars pressure difference exists from east to west, illustrating the possibility of a recharge to the system from east below 500 m u.s.l. Figure 10B shows the pressure distribution in the W-E trending cross-section C-C′.

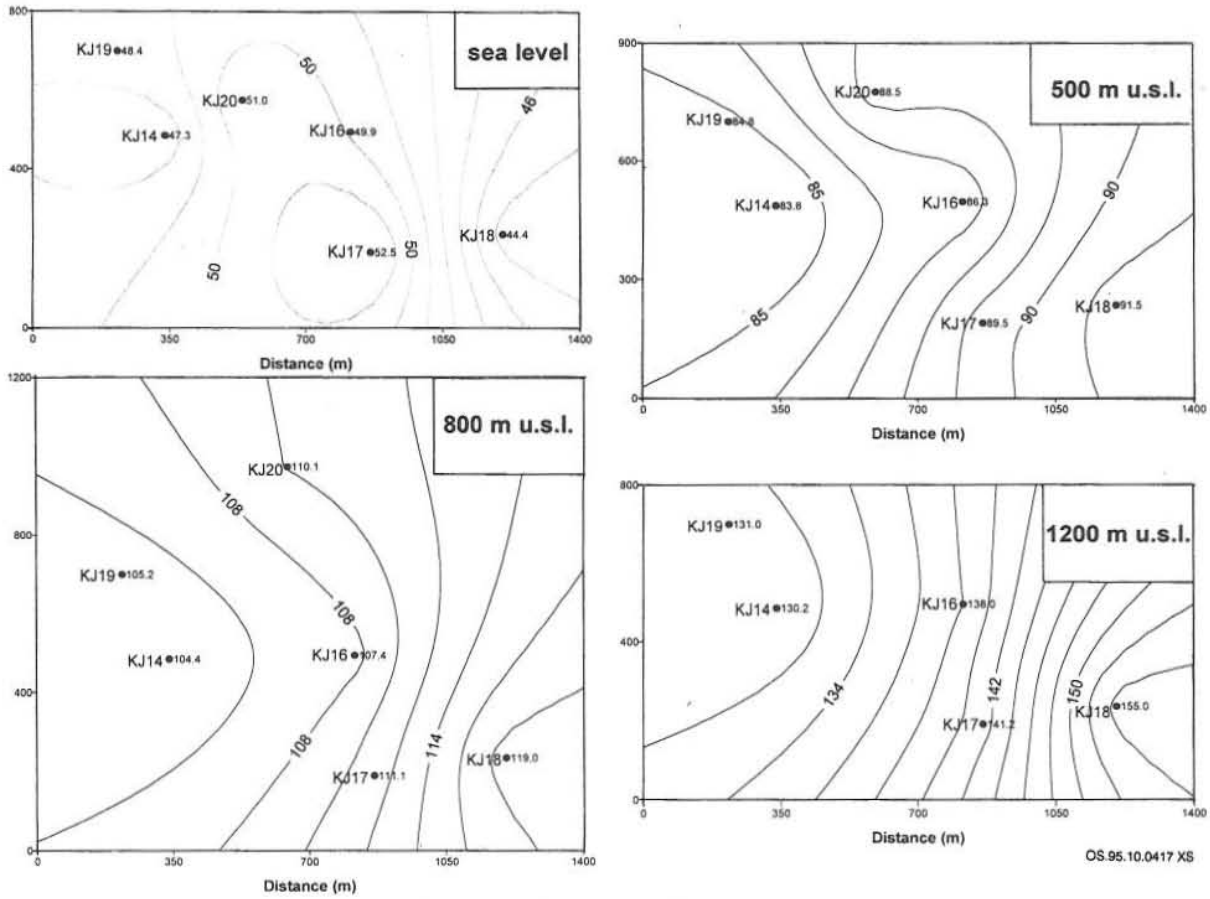


FIGURE 11: Iso-maps of the initial pressure distribution in the Sudurhlídar field

## 2.5 A conceptual reservoir model

Figure 12 presents a conceptual reservoir model for the Sudurhlídar field. The discontinuity in temperature and pressure across the fault $F_1$ demonstrates the impermeable and heat-isolating characteristics of this fault in its upper part and gives a distinct boundary of the geothermal field to the east. However, in its deeper part the temperature becomes more uniform. The observed pressure draw-down during the last 14 years in well KJ18 (see Appendix II) proves that relatively colder water recharges the reservoir from the east through the deeper part of $F_1$. This can explain the temperature anomaly at depth in the vicinity of wells KJ16 and KJ17, underneath a higher temperature two-phase system as shown in Figure 10.

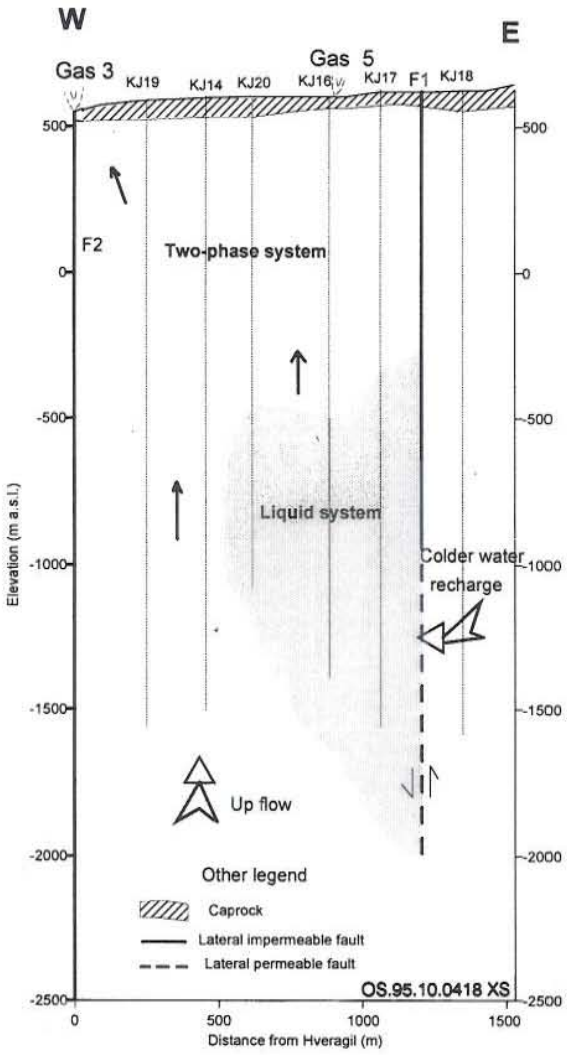


As mentioned in Chapter 1.1, the reservoir to the west of the Hveragil explosion craters along with the fault $F_2$ in its centre was contaminated by magmatic gases during the volcanic activity from 1975 to 1984, while it remained uncontaminated in the east. Furthermore, there exists a temperature and phase discontinuation between both sides of the Hveragil crater. From these phenomena the inference of the closed boundary nature of Hveragil craters and the fault $F_2$ is rational.

FIGURE 12: A natural state conceptual model for the Sudurhlídar geothermal system; the cross-section corresponds to the line C-C' in Figure 2

## 3. LUMPED PARAMETER MODELLING

This method of estimating the production capacity of a reservoir is analogous to methods used in electrical engineering. By considering the reservoir as a chain of zero-dimensional tanks that may connect with the surrounded reservoirs or tanks, and ignoring all of the spatial variations of the reservoir properties and fluid flow within the reservoir, a series of exponential equations have been derived. They describe the response and behaviour of the mean pressure change in a reservoir with time and discharge from the reservoir without being restricted by the boundary conditions. To tackle the simulation as an inverse problem, a powerful and effective programme LUMPFIT has been developed (Axelsson, 1985; 1989; Axelsson and Arason, 1992).

### 3.1 Production history

Production from the Sudurhlídar field began on 1980-09-19 when well KJ14 started to discharge. Wells KJ16, KJ17, KJ19 and KJ20 were put into production in 1981 and 1982. However, KJ16 has been closed since 1984, thus the pressure logging in this well should be the best one to reflect the change of the reservoir conditions. The other wells have continued to produce, but are closed for 3-5 months each summer except well KJ14. Table 3 gives the production history of the field in detail.

TABLE 3: Production history of the Sudurhlídar geothermal field

| From | To | KJ14 (kg/s) | KJ16 (kg/s) | KJ17 (kg/s) | KJ19 (kg/s) | KJ20 (kg/s) | Total flow (kg/s) |
|---|---|---|---|---|---|---|---|
| 19.09.1980 | 01.10.1980 | 25 | | | | | 25 |
| 01.10.1980 | 18.07.1981 | 15 | | | | | 15 |
| 18.07.1981 | 24.07.1981 | 15 | 17 | | | | 32 |
| 24.07.1981 | 01.08.1981 | 15 | 0 | | | | 15 |
| 01.08.1981 | 31.08.1981 | 14.5 | 9 | | | | 23.5 |
| 01.09.1981 | 01.10.1981 | 14 | 7.5 | | | | 21.5 |
| 02.10.1981 | 15.10.1981 | 13.5 | 7 | 17 | | | 37.5 |
| 15.10.1981 | 31.12.1981 | 13 | 6.5 | 10 | | | 29.5 |
| 01.01.1982 | 17.08.1982 | 12.5 | 6 | 9 | | | 27.5 |
| 17.08.1982 | 01.09.1982 | 12.5 | 6 | 9 | 17 | | 44.5 |
| 01.09.1982 | 05.10.1982 | 12.5 | 6.5 | 8.8 | 11 | | 38.8 |
| 05.10.1982 | 01.11.1982 | 14.8 | 6.5 | 8.8 | 9.5 | 22 | 61.6 |
| 01.11.1982 | 31.12.1982 | 14.8 | 6.5 | 8.8 | 9.5 | 14 | 53.6 |
| 01.01.1983 | 31.12.1983 | 13.2 | 5 | 9 | 9 | 10.8 | 47 |
| 01.01.1984 | 06.06.1984 | 13 | 4.5 | 9.3 | 9 | 10.8 | 46.6 |
| 06.06.1984 | 14.08.1984 | 12.5 | 0 | 0 | 0 | 0 | 12.5 |
| 14.08.1984 | 25.09.1984 | 12.5 | 0 | 14.1 | 9.5 | 11 | 47.1 |
| 25.09.1984 | 25.10.1984 | 12 | 6.5 | 14.1 | 9.5 | 10.5 | 52.6 |
| 25.10.1984 | 11.05.1985 | 11.5 | 0 | 14.1 | 9.5 | 10.5 | 45.6 |
| 11.05.1985 | 01.06.1985 | 11 | 0 | 0 | 0 | 0 | 11 |
| 01.06.1985 | 15.06.1985 | 11 | 7 | 0 | 0 | 0 | 18 |
| 15.06.1985 | 13.08.1985 | 11 | 0 | 0 | 0 | 0 | 11 |
| 13.08.1985 | 14.05.1986 | 11 | 0 | 12.6 | 9.5 | 10.5 | 43.6 |
| 14.05.1986 | 20.08.1986 | 10.5 | 0 | 0 | 0 | 0 | 10.5 |
| 20.08.1986 | 27.05.1987 | 10.5 | 0 | 12.6 | 9.5 | 10 | 42.6 |
| 27.05.1987 | 01.09.1987 | 10.5 | 0 | 0 | 0 | 0 | 10.5 |
| 01.09.1987 | 24.05.1988 | 11 | 0 | 10.2 | 8.5 | 8.5 | 38.2 |
| 24.05.1988 | 25.08.1988 | 11 | 0 | 0 | 0 | 0 | 11 |
| 25.08.1988 | 24.05.1989 | 10.5 | 0 | 10.1 | 7.5 | 9 | 37.1 |
| 24.05.1989 | 25.08.1989 | 10 | 0 | 0 | 0 | 0 | 10 |
| 25.08.1989 | 21.05.1990 | 10 | 0 | 10.9 | 7.5 | 11 | 39.4 |
| 21.05.1990 | 28.08.1990 | 10.5 | 0 | 0 | 0 | 0 | 10.5 |
| 28.08.1990 | 23.05.1991 | 11 | 0 | 9.6 | 8 | 9.5 | 38.1 |
| 23.05.1991 | 09.09.1991 | 0 | 0 | 0 | 0 | 0 | 0 |
| 09.09.1991 | 28.04.1992 | 10 | 0 | 10.4 | 7 | 12.3 | 39.7 |
| 28.04.1992 | 28.09.1992 | 10 | 0 | 0 | 0 | 0 | 10 |
| 28.09.1992 | 03.05.1993 | 9 | 0 | 11.5 | 6.5 | 9.2 | 36.2 |
| 03.05.1993 | 27.09.1993 | 9 | 0 | 0 | 0 | 0 | 9 |
| 27.09.1993 | 09.05.1994 | 9 | 0 | 14.3 | 6 | 8 | 37.3 |
| 09.05.1994 | 29.09.1994 | 8.3 | 0 | 0 | 0 | 0 | 8.3 |
| 29.09.1994 | 30.05.1995 | 9.6 | 0 | 11 | 6 | 8.5 | 35.1 |
| 30.05.1995 | 15.09.1995 | 9.6 | 0 | 0 | 0 | 0 | 9.6 |

### 3.2 Simulation

The pressure logging values at the major feedzone in well KJ16 are considered to represent the reservoir pressure. The pressure logging is carried out annually, generally at the end of the production stop that takes place in Krafla every summer. The production history was smoothed by taking the mean production value between two pressure measurements to correspond to the latter point, which means that the production in the year previous to the pressure measurement will influence the change in the reservoir pressure. Somehow, the observed pressure data seem not to reflect the production, no matter how the production data were treated. Therefore the production from the adjacent wells, KJ17 and KJ20, was also studied to check whether the pressure in well KJ16 is affected by only one well. The results deny the hypothesis, and are more or less similar to the simulation that use the total production. The data used to simulate the pressure history of well KJ16 are summarized in Table 4.

TABLE 4: Data used for the LUMPFIT simulation

| Time (month) | Production (kg/s) | | | Reservoir pressure (bar-g) |
|---|---|---|---|---|
| | Total | KJ17 | KJ20 | |
| 0.00 | 0.00 | 0.00 | 0.00 | 89.36 |
| 59.04 | 36.46 | 9.01 | 9.45 | 83.51 |
| 70.57 | 36.70 | 9.55 | 7.96 | 82.65 |
| 82.67 | 34.72 | 9.56 | 7.59 | 81.01 |
| 94.52 | 31.07 | 7.54 | 6.28 | 81.59 |
| 106.15 | 30.88 | 7.76 | 6.92 | 79.09 |
| 118.87 | 30.55 | 7.58 | 7.56 | 80.55 |
| 130.17 | 30.05 | 7.48 | 7.40 | 78.00 |
| 144.10 | 28.18 | 5.69 | 6.73 | 74.63 |
| 155.86 | 25.50 | 6.97 | 5.58 | 78.51 |
| 167.76 | 26.27 | 8.85 | 4.59 | 83.31 |
| 179.80 | 26.45 | 7.29 | 5.63 | 83.17 |

Table 5 shows the results of the lumped simulations. It is interesting to see in the simulations that when a few pressure points have been omitted, the coefficient of determination can be increased to 85% for open one-tank model while the fit curve does not change significantly, thus a rough estimation of the model properties is more or less valid. Figure 13 shows the fit curve for open one-tank model by using the total production. The calculated curve is governed by the following analytical equation which can be used to roughly predict the reservoir response to exploitation (Axelsson, 1989):

$$P(t) = P_i - \frac{10^{-5} Q}{\sigma_1} \left(1 - e^{\frac{-\sigma_1 t}{\kappa_1}}\right) \qquad (3)$$

where

$P(t)$ = Pressure in the reservoir (bar-g);
$P_i$ = Initial pressure in the reservoir (bar-g);
$Q$ = Production from the reservoir (kg/s);
$\sigma_1$ = Resistance to flow of water between tanks (ms);
$\kappa_1$ = Mass storage coefficient ($ms^2$);
$t$ = Time from September 1980 (s).

TABLE 5: A summary of lumped simulation for the Sudurhlídar geothemal field (R.m.s. = Root mean squared)

| Model type | Total production history | | KJ17 production history | | KJ20 production history | |
|---|---|---|---|---|---|---|
| | closed one-tank | open one-tank | closed one-tank | open one-tank | closed one-tank | open one-tank |
| Coeff. of deter. (%) | 0 | 24 | 27 | 55 | 36 | 62 |
| R.m.s. misfit (bars) | 3.26 | 2.31 | 3 | 2.37 | 2.82 | 2.16 |
| Standard deviation (bars) | 3.11 | 2.55 | 3.14 | 2.6 | 2.94 | 2.37 |
| $\kappa_1$ ($10^3$ ms$^2$) | 12.44 | 5.5 | 3.23 | 1.5 | 3.06 | 1.44 |
| $B$ ($10^{-3}$) | 2.12 | | 8.17 | | 8.6 | |
| $\sigma_1$ ($10^{-6}$ ms) | | 28.74 | | 7.09 | | 6.47 |
| $A_1$ ($10^{-3}$) | | 4.79 | | 17.63 | | 18.29 |
| $L_1$ ($10^{-3}$) | | 13.77 | | 12.49 | | 11.83 |

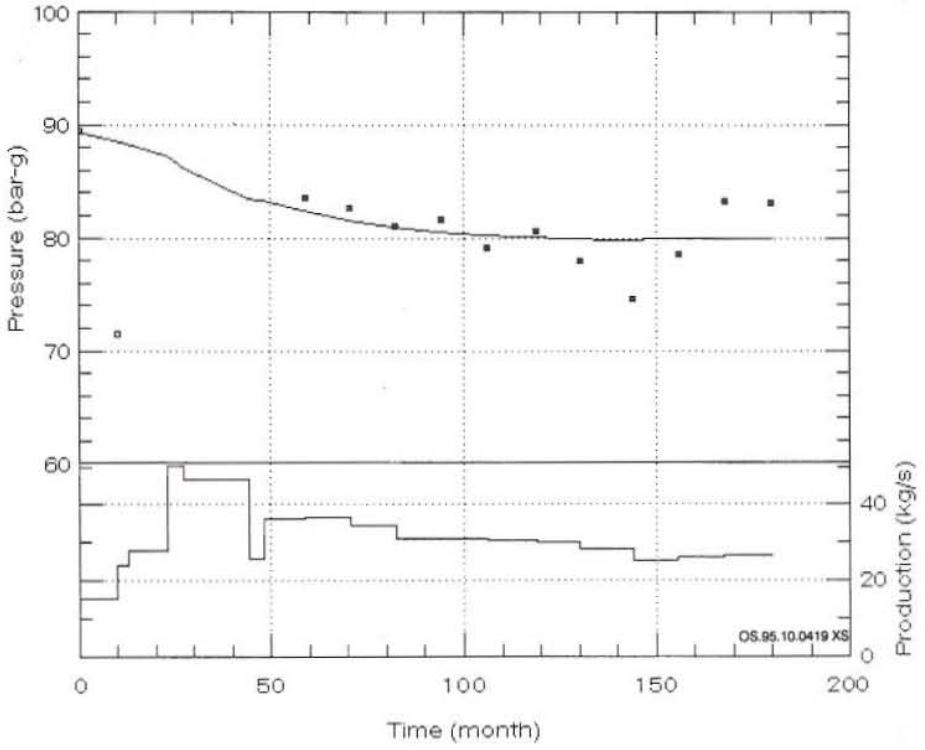


FIGURE 13: A comparison of measured and calculated pressure data in well KJ16 for one-tank open model, and the total production of the Sudurhlídar field

### 3.3 Evaluation of the reservoir size

The properties of the lumped model described above can be used for estimating the reservoir volume that is influenced by production from the Sudurhlídar wells. The relation between the reservoir volume and the lumped model storage coefficient $\kappa_1$ is given by (Axelsson, 1989)

$$V = \frac{\kappa_1}{S} \tag{4}$$

where

$V$ = Reservoir volume ($m^3$);
$S$ = Storativity ($kg/m^3p_a$).

Because of the thin caprock assumed for the Sudurhlídar reservoir, both confined and unconfined liquid-dominated reservoir conditions have to be considered. The storativity for a confined reservoir is

$$S = \rho_w (\phi\beta + (1-\phi)\alpha) \quad (5)$$

where

$\rho_w$ = Fluid density ($kg/m^3$);
$\phi$ = Rock porosity, assumed $\phi$=0.085;
$\beta$ = Fluid compressibility ($Pa^{-1}$);
$\alpha$ = Rock compressibility ($Pa^{-1}$), assumed as $1.33 \times 10^{-11}$ $Pa^{-1}$ for basalt,

while the storativity for an unconfined reservoir is given by:

$$S = \frac{\phi}{g H} \quad (6)$$

where

$g$ = Acceleration of gravity ($m/s^2$), assumed as 9.8 $m/s^2$;
$H$ = Reservoir thickness (m), assumed as 2500 m.

Table 6 shows the results of the evaluation. The reservoir area ranges between 0.6 to 15.6 $km^2$.

TABLE 6: Estimated reservoir area and volume based on lumped modelling

| Property | Confined reservoir | Unconfined reservoir | Mean value |
|---|---|---|---|
| Storativity ($10^{-7}$ $kg/m^3Pa$) | 1.415 | 34.7 | |
| Reservoir volume ($km^3$) | 38.9 | 1.59 | 20.3 |
| Reservoir area ($km^2$) | 15.55 | 0.63 | 8.1 |

Combining this with the resistivity investigation and exploitation history, a value around 10 $km^2$ is suggested as a possible size of the geothermal area.

## 4. GEOTHERMAL RESERVE ASSESSMENT

### 4.1 Governing equations

The geothermal reserve of a field can be roughly estimated by employing a volumetric method. The "stored heat" in the homogenous and totally closed reservoir is defined by the following equation (Sarmiento, 1993):

$$E = V\rho_r C_r (1-\phi)(T - T_r) + V\rho_f \phi (h_f - h_r) \quad (7)$$

where

$E$ = Stored heat in the reservoir (kJ);
$V$ = Reservoir volume ($m^3$);
$\rho_r$, $\rho_f$ = Density of rock and fluid ($kg/m^3$);
$C_r$ = Heat capacity of rock;
$T$, $T_r$ = Initial reservoir temperature and the final reference temperature (°C);
$\phi$ = Porosity of rock (%);
$h_f$, $h_r$ = Initial fluid enthalpy in the reservoir and at the final reference temperature (kJ/kg).

The equation that applies for converting the heat reserve into electrical power is given as:

$$Reserve\ (MW_e) = \frac{E * Recovery\ factor * Conversion\ efficiency}{Plant\ load * Load\ factor} \quad (8)$$

A power corresponding to 12 $MW_e$ has already been extracted from the field during the last 14 years, yet no dramatic pressure draw-down or temperature cooling have been observed in the reservoir. This may indicate a larger reservoir. Therefore the enclosure of the extensive proven reservoir as shown in Figure 2 is quite reasonable. In order to deal with some uncertainty in reservoir parameters, a method called Monte Carlo has also been carried out (Sarmiento, 1993).

### 4.2 Volumetric assessment

The saturation of steam at initial state is very difficult to determine. An assumption of zero saturation is considered both because the hydrostatic pressure dominates in the reservoir, and because the ratio of the stored heat contained in the fluid is much lower compared with those contained in the rock. So the neglect of the steam will vaguely affect the assessment. The temperature in the reservoir is not uniform, therefore the reservoir volume has been divided into several sub-blocks as shown in Figure 14, in order to get a more precise reserve estimate.

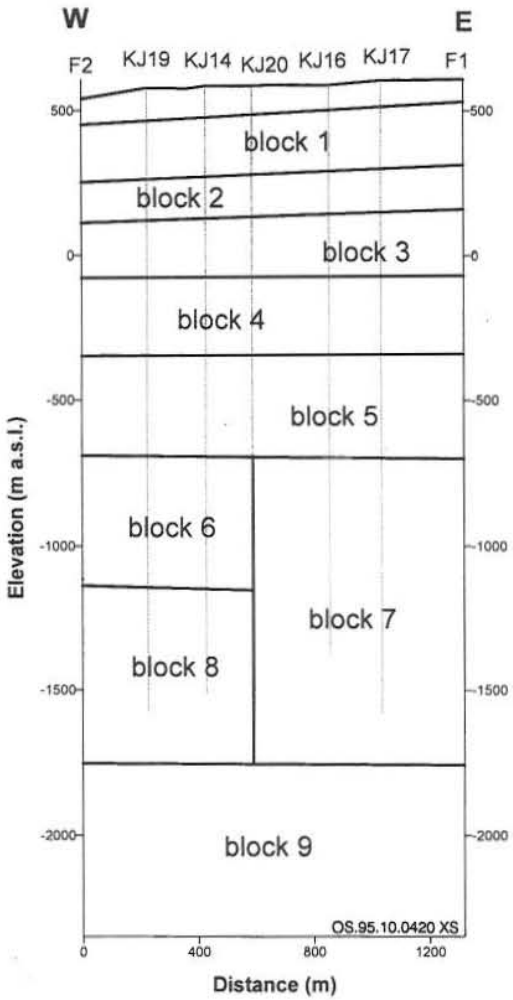


FIGURE 14: The reservoir volume divided into sub-blocks for volumetric assessment

The reference temperature, that is the temperature when production from wells is terminated, is chosen at 180°C since the saturated fluid from wells is separated at 8 bars in the power plant. Correspondingly, the reference water enthalpy is fixed. The electrical converting parameters such as conversion efficiency, plant load and load factor are assumed to be constant according to the experience. All the parameters used for the proven area are summarized in Table 7. Table 8 shows the results of the calculations for each block. From the calculation a result of 22 $MW_e$ reserve for 30 years production is proposed for the proven area.

TABLE 7: Parameters used for volumetric assessment in the proven Sudurhlídar area

| Parameter | Unit | Value | Parameter | Unit | Value |
|---|---|---|---|---|---|
| Area | $km^2$ | 1.3 | Recovery factor | % | 15 |
| Rock density | $kg/m^3$ | 2800 | Conversion efficiency | % | 9 |
| Rock porosity | % | 5 | Load plant factor | % | 80 |
| Rock heat capacity | kJ/kg°C | 1 | Plant life | year | 30 |

TABLE 8: Volumetric calculations in individual blocks (see Figure 14)

| Block number | Thickness (m) | Temperature (°C) | Water enthalpy (kJ/kg) | Water density ($kg/m^3$) | Area ($km^2$) | $MW_e$ |
|---|---|---|---|---|---|---|
| 1 | 200 | 205 | 875 | 860 | 1.3 | 0.34 |
| 2 | 140 | 240 | 1040 | 814 | 1.3 | 0.56 |
| 3 | 190 | 260 | 1135 | 784 | 1.3 | 1.01 |
| 4 | 290 | 280 | 1235 | 750 | 1.3 | 1.91 |
| 5 | 340 | 300 | 1405 | 712 | 1.3 | 2.71 |
| 6 | 435 | 320 | 1460 | 667 | 0.65 | 2.09 |
| 7 | 1065 | 280 | 1235 | 750 | 0.65 | 3.52 |
| 8 | 610 | 340 | 1595 | 610 | 0.65 | 3.20 |
| 9 | 600 | 355 | 1745 | 538 | 1.3 | 6.86 |

### 4.3 Volumetric assessment by Monte Carlo method

The Monte Carlo reservoir assessment method applies when critical factors in the reserve equation (Equation 8) are only known as uncertainty. As an example the drilling in the Sudurhlídar field has covered only a reservoir area of 1.3 $km^2$, which is here considered as a proven reservoir area. If other data such as the subsurface resistivity and the lumped volume are also taken into account, a much larger reserve may exist. Thus we also have a possible reservoir area to consider. Furthermore, properties like porosity and initial reservoir temperature may vary. Therefore the method assumes that some or all of the properties in Equation 8 have some random character (constant, square and triangular).

The uncertain parameters in the reservoir are presented in Table 9. Under an "EXCEL spread sheet", 8x2000 matrix has been created both for the proven and the possible area. Each line of the matrix is used for calculating a single reserve, according to Equation 8.

The 2000 reserve calculations performed by the EXCEL spread sheet are finally shown as histograms in Figure 15. They illustrate that the power potential of the Sudurhlídar field is between 15 and 35 $MW_e$ for the proven area and between 30 and 70 $MW_e$ for the possible area.

TABLE 9: Volumetric assessment parameters and their probability distribution in the Sudurhlídar geothermal field

| Property | Unit | Best guess | Probability distribution | | |
|---|---|---|---|---|---|
| | | | Type | From | To |
| Proven area | $km^2$ | 3 | Triangular | 1.5 | 4.5 |
| Possible area | $km^2$ | 7 | Triangular | 5 | 10 |
| Proven reservoir thickness | m | 2000 | Triangular | 1500 | 2500 |
| Possible reservoir thickness | m | 2500 | Triangular | 2000 | 3000 |
| Rock density | $kg/m^3$ | 2800 | Square | 2600 | 3100 |
| Rock porosity | % | 5 | Triangular | 2 | 15 |
| Water density | $kg/m^3$ | 732.118 | Square | 574.35 | 783.94 |
| Reservoir temperature | °C | 290 | Square | 230 | 350 |
| Water enthalpy | kJ/kg | 1290 | Square | 1134.9 | 1671.9 |
| Rock heat capacity | kJ/kg°C | 1 | Constant | --- | --- |
| Reference temperature | °C | 180 | Constant | --- | --- |
| Reference water enthalpy | kJ/kg | 762.12 | Constant | --- | --- |
| Recovery factor | % | 15 | Square | 10 | 20 |
| Conversion efficiency | % | 9 | Constant | --- | --- |
| Load plant factor | % | 80 | Constant | --- | --- |
| Plant life | year | 30 | Constant | --- | --- |

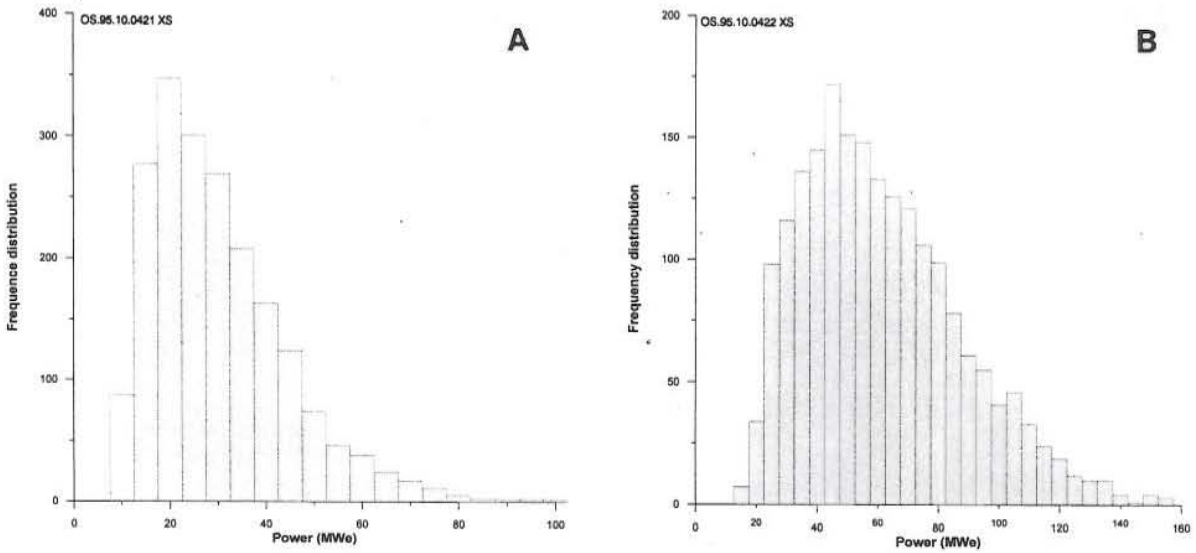


FIGURE 15: Frequency distribution for the potential electric power, a) for the proven reservoir; b) for the possible reservoir

## 5. CONCLUSIONS

The main conclusions of this study are:

1. The Sudurhlídar geothermal field was, in its natural state, mostly filled with boiling liquid water. The fractured reservoir is at least partially confined due to the caprock characteristics. The temperature in the reservoir ranges from 230 to 350°C, and follows chiefly the boiling point depth curve.

2. The pressure distribution in the reservoir is a function of the temperature, and is described by Equation 1 (see Chapter 2.4). Two N-S faults $F_1$ and $F_2$ which are both laterally impermeable, close the system to the east and to the west. However, along the deeper parts of $F_1$ it becomes permeable and relatively "cold" water, at 250°C, penetrates into the reservoir and forms a liquid system at 1000-2000 m depth in the eastern part of the field by mixing with and condensing the up-flowing boiling fluid from depth.

3. The observed reservoir pressure seems not to correspond accurately to the production. This is most probably caused by either the fractured nature, or the boiling in the reservoir. Still the lumped parameter modelling allows estimation of the following:

   a. The pressure in the reservoir will behave according to the following equation:

$$P(t) = 89.36 - 0.3526\, Q\, (1 - e^{-5.2255 \times 10^{-9}\, t}) \qquad (9)$$

   where the symbols are defined the same as Equation 2 in Chapter 3.2.

   b. The reservoir area is around 10 km$^2$.

4. Volumetric method was employed to assess the geothermal reserve of the Sudurhlídar field. Assuming 30 years of operation for the proven area of 1.3 km$^2$, a 22 MW$_e$ power potential is proposed. To handle some uncertainty reservoir parameters, the Monte Carlo method has also been used. The frequency distribution of this study shows that for the proven area, a 15-35 MW$_e$ reserve is available, while for the possible area, a 20-60 MW$_e$ reserve is hopeful for a plant operation for 30 years.

## ACKNOWLEDGEMENTS

I would like to thank my advisors Grímur Björnsson and Benedikt Steingrímsson for their valuable and unselfish guidance and help. I would express my thanks to the lecturer staff who offer their precious knowledge to us during the training programme. Also thanks to the drawing ladies in Orkustofnun for completing some of my figures. Special thanks to Ingvar B. Fridleifsson and Lúdvík S. Georgsson, directors of the UNU Geothermal Training Programme, for supplying me with such a good opportunity to learn the most advanced geothermal knowledge in the world and also for their excellent guidance and management. Also, thanks go to Margrét Westlund and Súsanna Westlund for their support during my stay in Iceland. Finally, I appreciate the directors of my institute, who allowed me to attend the training.

## REFERENCES

Arason, P., and Björnsson, G., 1994: *ICEBOX.*. 2nd edition, Orkustofnun, Reykjavík, 38 pp.

Ármannsson, H., Benjamínsson, J., and Jeffrey, A.W.A., 1989: Gas changes in the Krafla geothermal system, Iceland. *Geochemical Geology, 76,* 175-196.

Ármannsson, H., Gudmundsson, Á., and Steingrímsson, B.S., 1987: Exploration and development of the Krafla geothermal area. *Jökull, 37*, 12-29.

Árnason, K., and Flóvenz, Ó.G., 1992: Evaluation of physical methods in geothermal exploration of rifted volcanic crust. *Geoth. Res. Council, Transactions, 16*, 207-214.

Árnason, K., and Karlsdóttir, R., 1995: *Resistivity survey in the Krafla area.* Orkustofnun, Reykjavík, report in print (in Icelandic), 97 pp.

Axelsson, G., 1985: *Hydrology and thermomechanics of liquid-dominated hydrothermal systems in Iceland.* Ph.D. thesis, Oregon State University, Corvallis, Oregon, 291 pp.

Axelsson, G., 1989: Simulation of pressure response data from geothermal reservoirs by lumped parameter models. *Proceedings of the 14th Workshop on Geothermal Reservoir Engineering*, Stanford University, Ca., 257-263.

Axelsson, G., and Arason, P., 1992: *LUMPFIT, automated simulation of pressure changes in hydrological reservoirs. Version 3.1, user's guide*. Orkustofnun, Reykjavík, 32 pp.

Bödvarsson, G.S., Pruess, K., Stefánsson, V., and Elíasson, E.T., 1984: The Krafla geothermal field, Iceland, 2. Natural state of the system. *Water Resources Research, 20-11*, 1531-1544.

Helgason, P., 1993: *Step by step guide to BERGHITI. User's guide.* Orkustofnun, Reykjavík, 17 pp.

Sarmiento, Z.F., 1993: *Geothermal development in the Philippines*. UNU G.T.P., Iceland, report 2, 99 pp.

Stefánsson, V., 1981: The Krafla geothermal field, northeast Iceland. In: Rybach, L., and Muffler, L.J.P. (editors), *Geothermal systems: Principles and case histories*. John Wiley and Son Ltd., Chichester, 273-294.

## APPENDIX I: Formation temperature estimation in well KJ19 by the Albright method

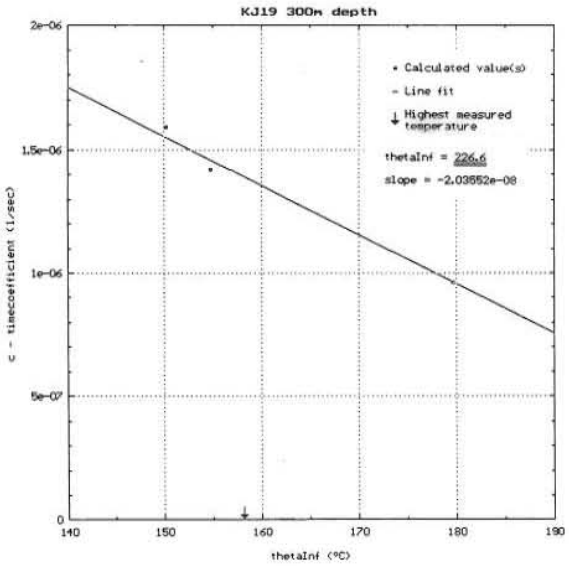


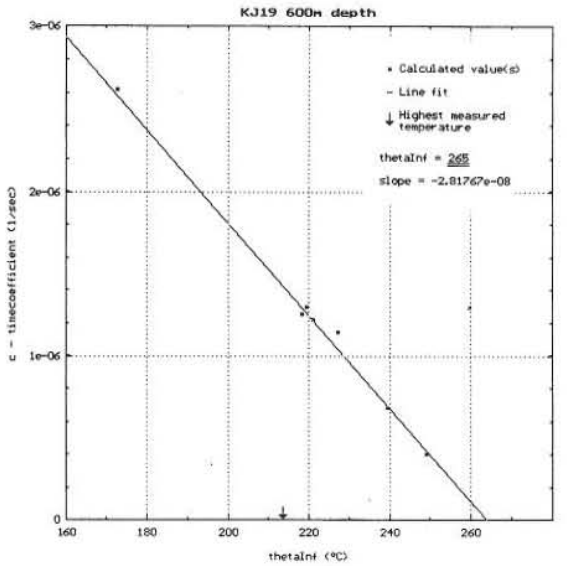


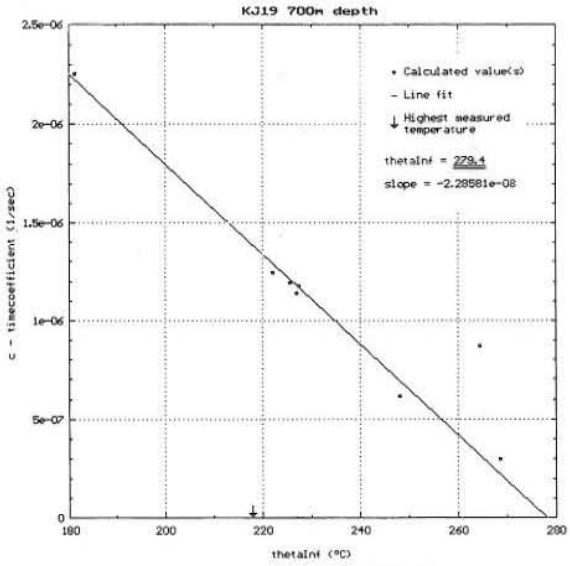


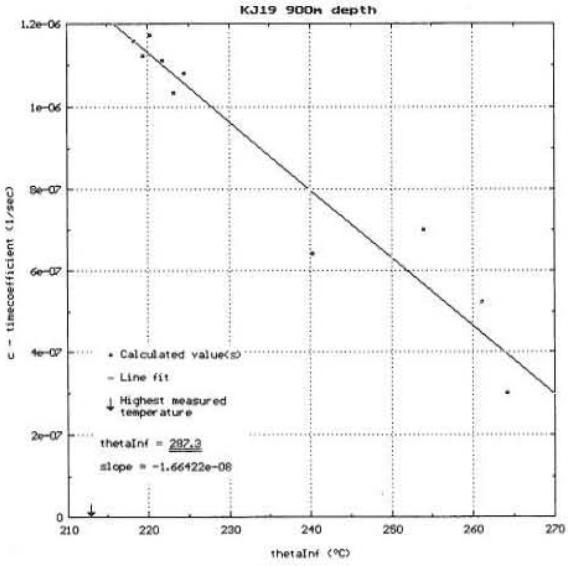


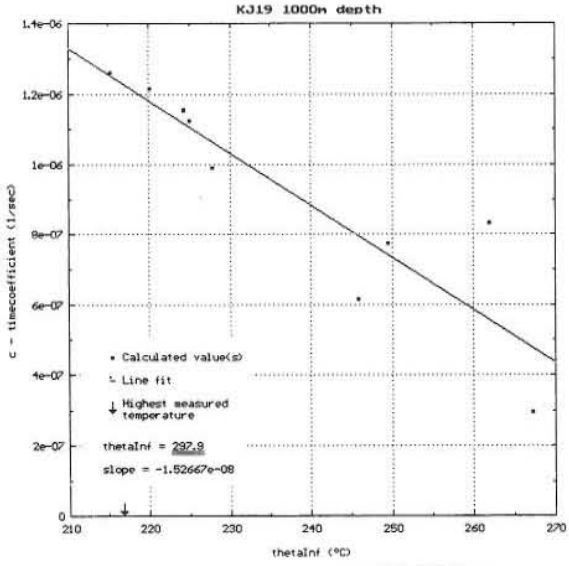


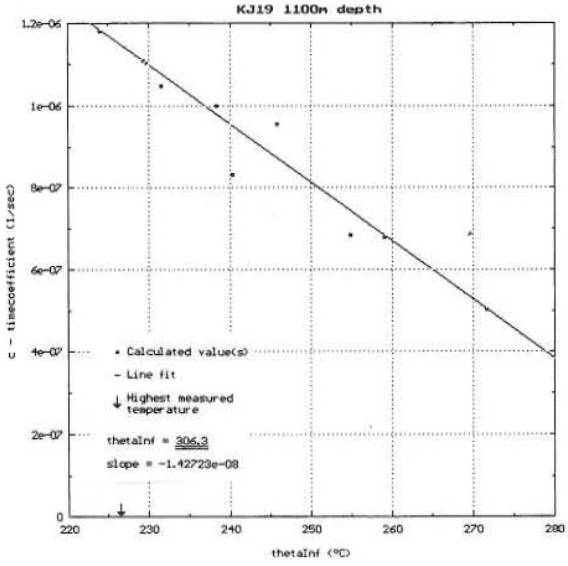

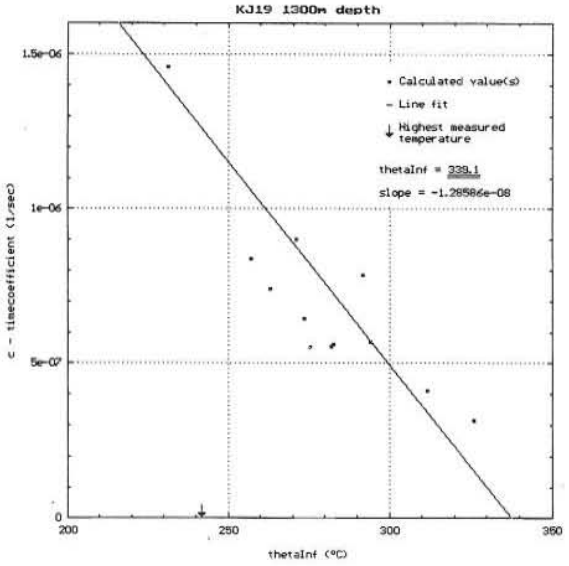
KJ19 1300m depth
* Calculated value(s)
- Line fit
↓ Highest measured temperature
thetaInf = 339.1
slope = -1.28586e-08
c - tinecoefficient (1/sec)
thetaInf (°C)

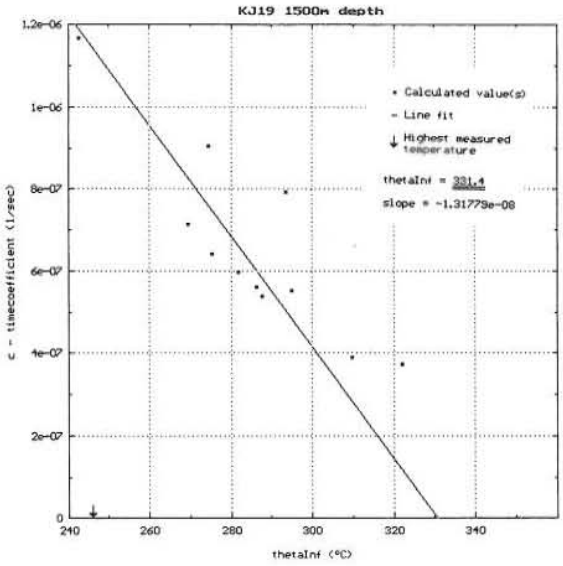
KJ19 1500m depth
* Calculated value(s)
- Line fit
↓ Highest measured temperature
thetaInf = 331.4
slope = -1.31779e-08
c - tinecoefficient (1/sec)
thetaInf (°C)

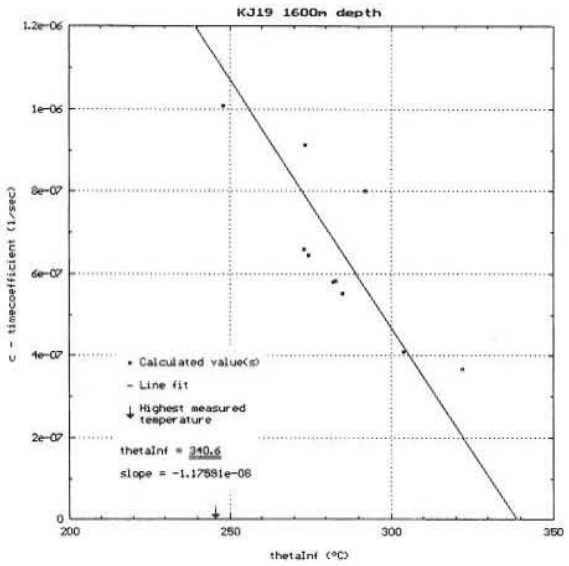
KJ19 1600m depth
* Calculated value(s)
- Line fit
↓ Highest measured temperature
thetaInf = 340.6
slope = -1.17881e-08
c - tinecoefficient (1/sec)
thetaInf (°C)

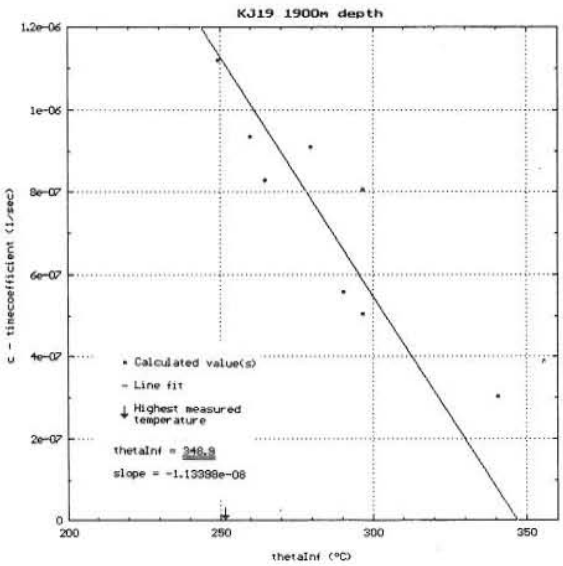
KJ19 1900m depth
* Calculated value(s)
- Line fit
↓ Highest measured temperature
thetaInf = 348.9
slope = -1.13398e-08
c - tinecoefficient (1/sec)
thetaInf (°C)

## APPENDIX II: Downhole pressure and temperature measurements in wells in the Sudurhlídar geothermal field

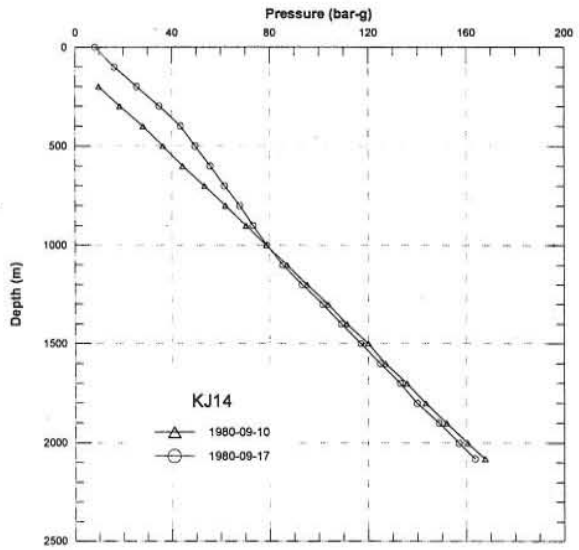


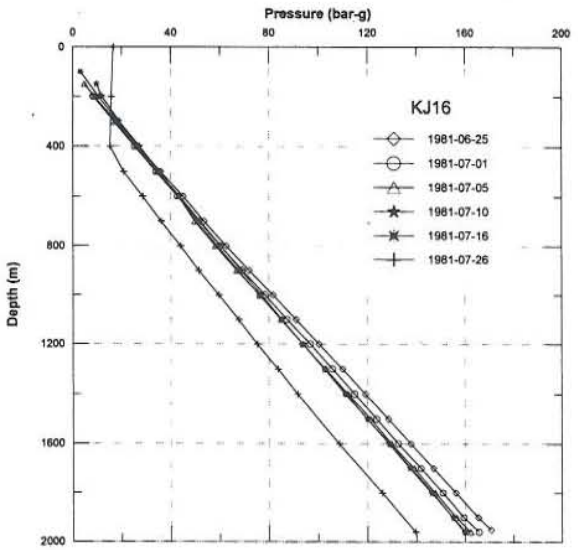


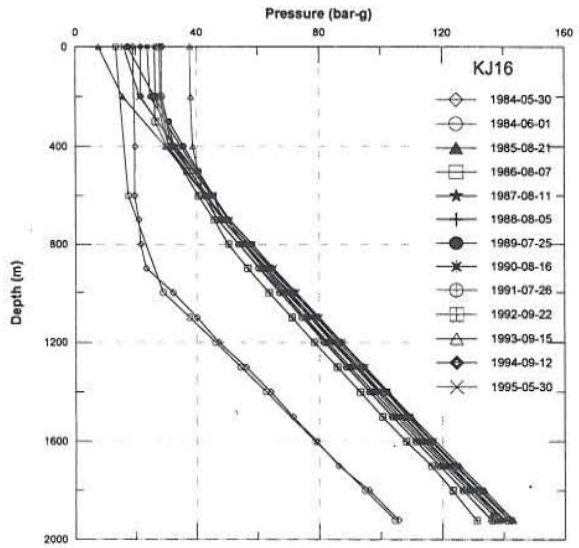


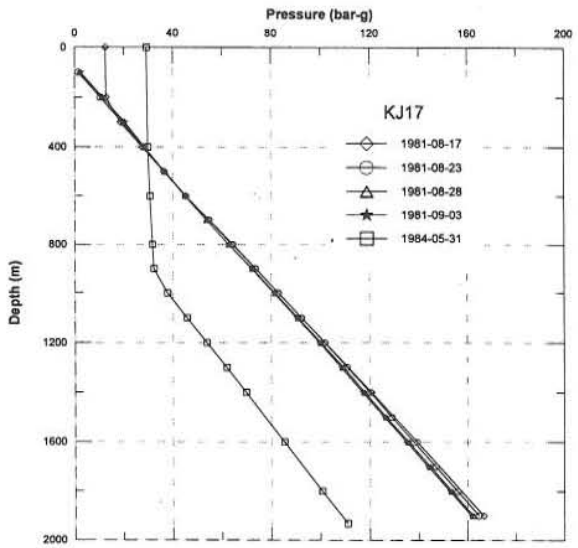


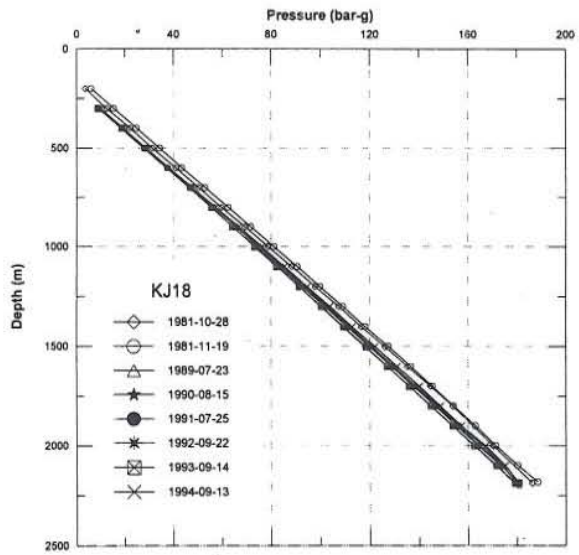


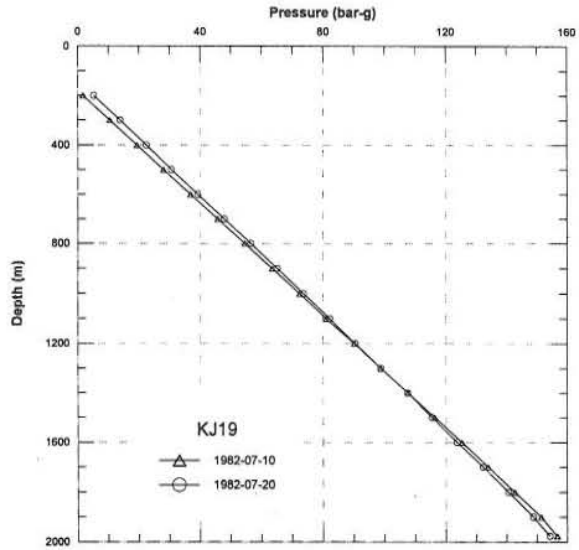

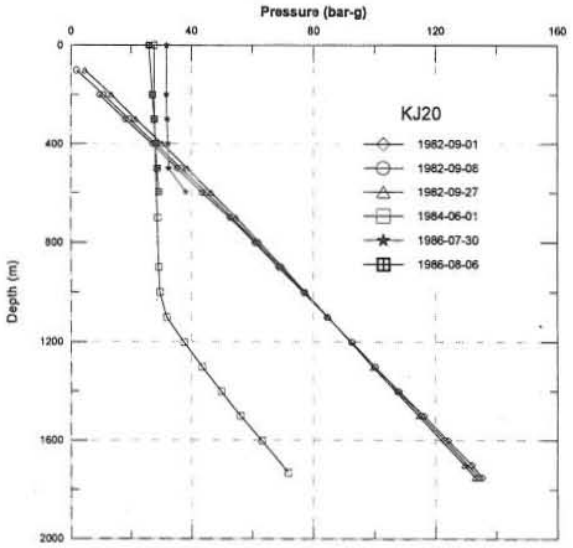
Pressure (bar-g)
0
40
80
120
160
Depth (m)
0
400
800
1200
1600
2000
KJ20
1982-09-01
1982-09-08
1982-09-27
1984-06-01
1986-07-30
1986-08-06

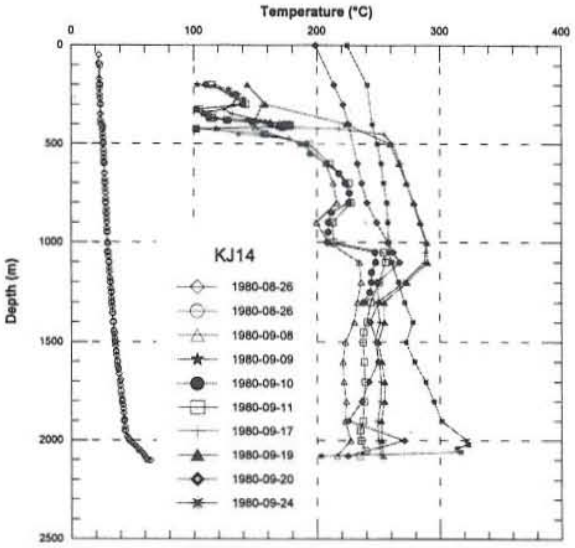
Temperature (°C)
0
100
200
300
400
Depth (m)
0
500
1000
1500
2000
2500
KJ14
1980-08-26
1980-08-26
1980-09-08
1980-09-09
1980-09-10
1980-09-11
1980-09-17
1980-09-19
1980-09-20
1980-09-24

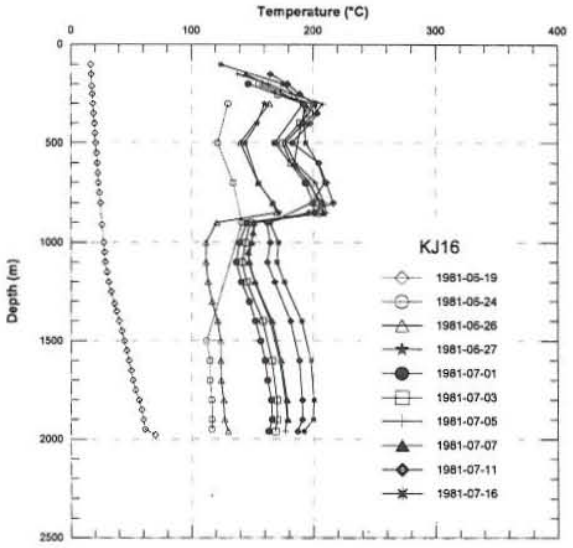
Temperature (°C)
0
100
200
300
400
Depth (m)
0
500
1000
1500
2000
2500
KJ16
1981-05-19
1981-05-24
1981-06-26
1981-06-27
1981-07-01
1981-07-03
1981-07-05
1981-07-07
1981-07-11
1981-07-16

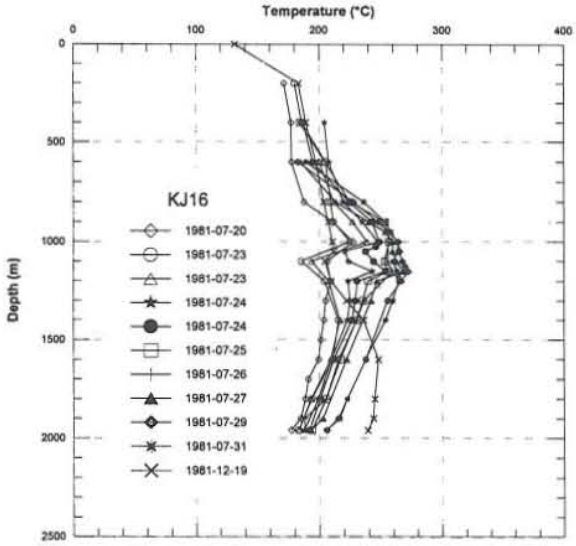
Temperature (°C)
0
100
200
300
400
Depth (m)
0
500
1000
1500
2000
2500
KJ16
1981-07-20
1981-07-23
1981-07-23
1981-07-24
1981-07-24
1981-07-25
1981-07-26
1981-07-27
1981-07-29
1981-07-31
1981-12-19

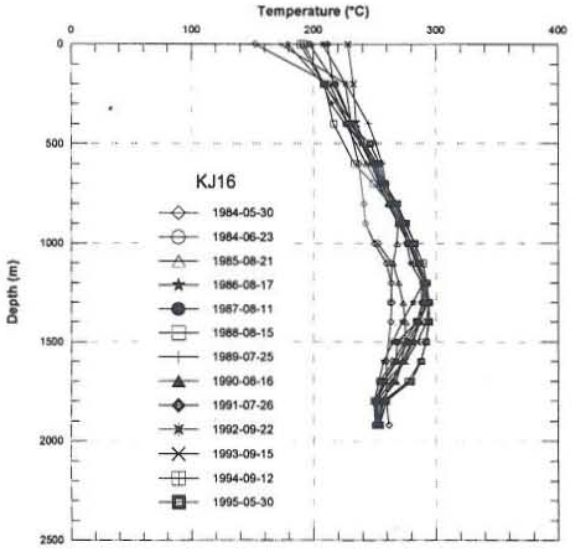
Temperature (°C)
0
100
200
300
400
Depth (m)
0
500
1000
1500
2000
2500
KJ16
1984-05-30
1984-06-23
1985-08-21
1986-08-17
1987-08-11
1988-08-15
1989-07-25
1990-08-16
1991-07-26
1992-09-22
1993-09-15
1994-09-12
1995-05-30

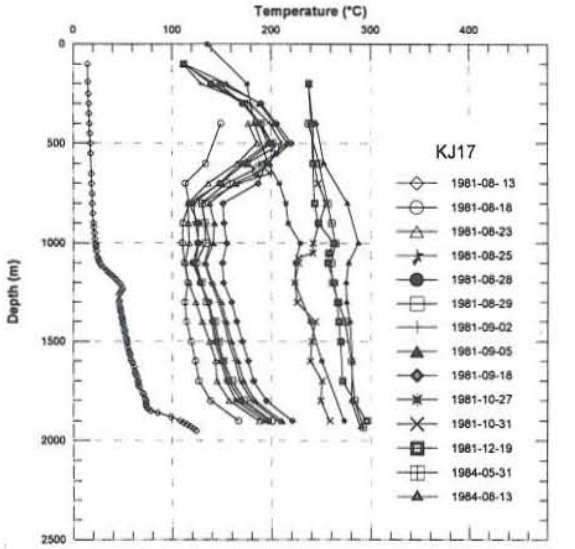
Temperature (°C)
0
100
200
300
400
Depth (m)
0
500
1000
1500
2000
2500
KJ17
1981-08- 13
1981-08-18
1981-08-23
1981-08-25
1981-08-28
1981-08-29
1981-09-02
1981-09-05
1981-09-18
1981-10-27
1981-10-31
1981-12-19
1984-05-31
1984-08-13

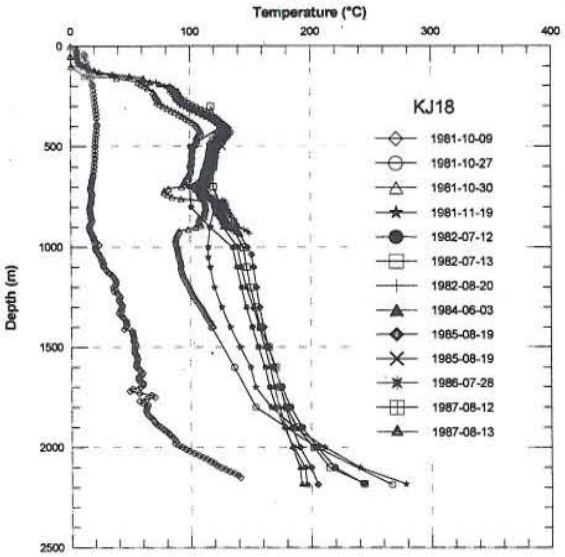
Temperature (°C)
Depth (m)
KJ18
1981-10-09
1981-10-27
1981-10-30
1981-11-19
1982-07-12
1982-07-13
1982-08-20
1984-06-03
1985-08-19
1985-08-19
1986-07-28
1987-08-12
1987-08-13

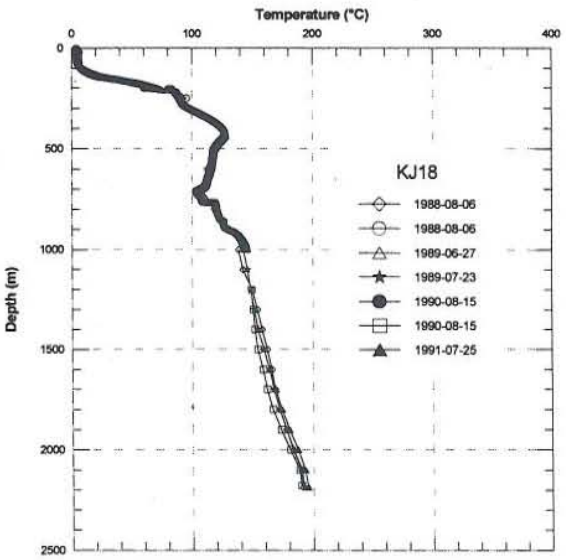
Temperature (°C)
Depth (m)
KJ18
1988-08-06
1988-08-06
1989-06-27
1989-07-23
1990-08-15
1990-08-15
1991-07-25

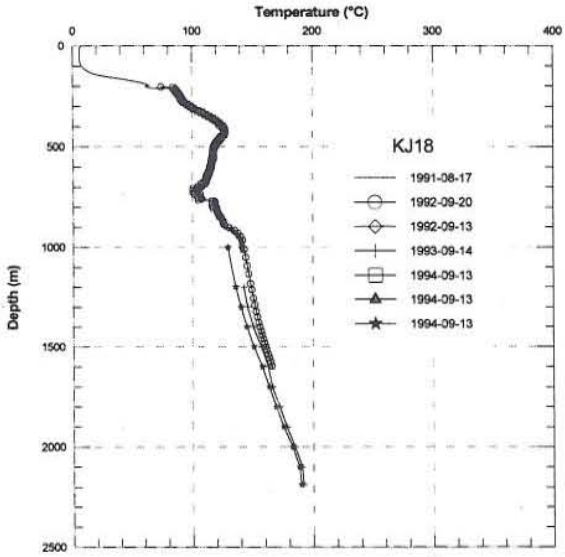
Temperature (°C)
Depth (m)
KJ18
1991-08-17
1992-09-20
1992-09-13
1993-09-14
1994-09-13
1994-09-13
1994-09-13

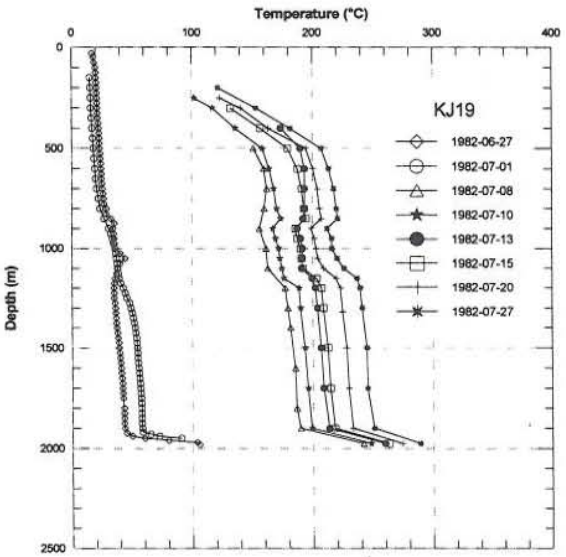
Temperature (°C)
Depth (m)
KJ19
1982-06-27
1982-07-01
1982-07-08
1982-07-10
1982-07-13
1982-07-15
1982-07-20
1982-07-27

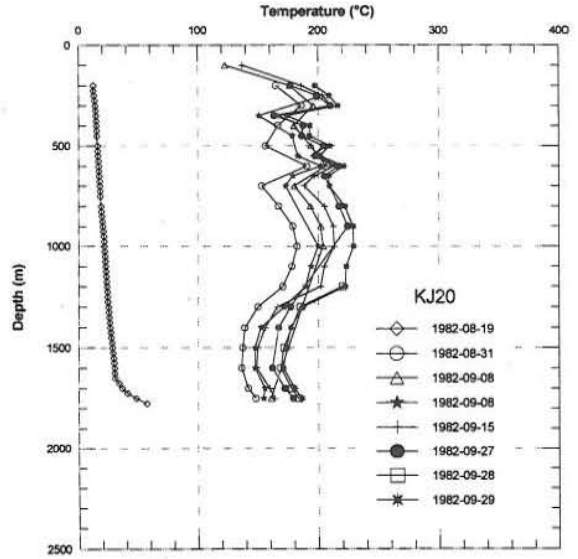
Temperature (°C)
Depth (m)
KJ20
1982-08-19
1982-08-31
1982-09-08
1982-09-08
1982-09-15
1982-09-27
1982-09-28
1982-09-29

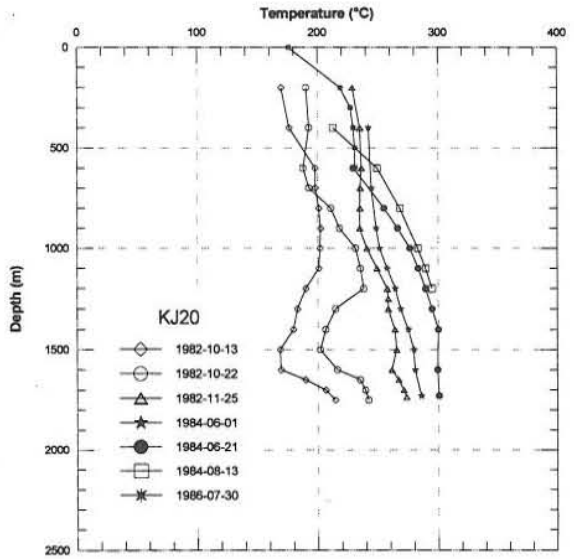
Temperature (°C)
Depth (m)
KJ20
1982-10-13
1982-10-22
1982-11-25
1984-06-01
1984-06-21
1984-08-13
1986-07-30